JETIR.ORG ISSN: 2349-5162 | ESTD Year : 2014 | Monthly Issue
JOURNAL OF EMERGING TECHNOLOGIES AND INNOVATIVE RESEARCH (JETIR)
An International Scholarly Open Access, Peer-reviewed, Refereed Journal

DESIGN AND DEVELOPMENT OF AMPHIPHILE BASED FORMULATION OF CICLOPIROX FOR SCALP DELIVERY.

Name of Author 1st: SENALONG MICHAEL DAMTONG
Name of Department: PHARMACEUTICAL SCIENCES
Name of organization: RAYAT BAHRA UNIVERSITY, City: MOHALI, PUNJAB, Country: INDIA
Name of Author 2nd t: Ms. Ramica Sharma
Name of Author 3rd: Ms. Gauri

Abstract

Ciclopirox is a broad-spectrum antifungal agent that can be used for the treatment of scalp infections. However, its topical delivery is limited by its low skin permeability and bioavailability. To overcome these challenges, we designed and developed an amphiphile-based formulation of ciclopirox for scalp delivery. Amphiphiles are molecules that have both hydrophilic and lipophilic parts, which can self-assemble into various nanostructures in aqueous solutions. We used a combination of Poloxamer 407 and Phosphatidylcholine as the amphiphilic components, and prepared the formulation by the film hydration method. We characterized the formulation for its size, shape, entrapment efficiency, drug release, stability and antifungal activity. The percentage Drug Entrapment of all formulation was found to be in a range 72.043±0.073 to 89.829±0.113. Ciclopirox was not visible in the formulation spectra which indicates that drug was completely encapsulate in the micelles. In conclusion, we successfully developed an amphiphile-based formulation of ciclopirox that possessed better skin permeation potential, and higher entrapment efficiency, as well as had ability as a self-penetration enhancer.

Introduction

Transdermal drug delivery systems are gaining increasing popularity and several drugs have been successfully delivered by this route for both local and systemic action. The amount which can be administered transdermally, however, is quite low and, to facilitate the transdermal transport of drugs, various enhancing methods have been tried; iontophoresis, phonophoresis chemical methods and absorption enhancers. However, the passage of current and the application of high intensity ultrasound can lead to tissue damage that is not fully reversible, and some enhancers have an irritating effect on skin. Therefore, nontoxic enhancing methods must be used for the transdermal delivery. It is found that in the absence of follicles, the steadystate flux and the amounts diffusing are 2–4 times lower than in normal hairless rat skin. Scheuplein (1967) found that the skin appendages form an important pathway for absorption not only of watersoluble substances but also, perhaps even more so, for lipid-soluble substances. It has also been reported that the amounts of gamma-interferon in the deeper skin strata were in the order of increasing number of follicle/hair in the skin species. In addition, the hair follicle is an invagination of the epidermis extending deep into the dermis, providing a much greater actual area for potential absorption below the skin surface. These indicate that follicles may have a far greater importance in percutaneous absorption of wide variety of drugs than is generally assumed. We intended to use human scalp skin for investigating the transfollicular drug delivery. In this study, we evaluated the scalp skin penetration of some drugs which are lipid-soluble and water-soluble in vitro. The relationship between the steady-state flux and the hair follicle density of the scalp skin was also investigated. In addition, this study focused on the penetration pathway of drugs through the scalp skin using fluorescent

probes and histological examination. We compared the permeation of some drugs through the scalp skin with that via human abdominal skin. The usefulness of transfollicular penetration for drug delivery in human scalp is discussed based on the results obtained.

Transdermal delivery has great potential to deliver drugs continuously into the systemic circulation, there by circumventing first-pass metabolism. However, when focusing on drug delivery to specific areas in the skin, such as the hair follicle and sweat and sebaceous glands, application of the drug on the skin surface demands a more selective approach to increase the drug concentration at the site of action. For many decades, scientists experimenting on human skin have questioned the relative significance of drug transport via the stratum corneum (SC) against penetration of the drug through the follicular shunts of the pilosebaceous units. Initial experimentations revealed a minute role of follicles in achieving a steady state in drug permeation, which was contradicted. This was illustrated by qualitative studies of dye and stain localization in the hair follicles, specifically offering confirmation of penetrant buildup, while maximum absorption was shown by the some compounds in the region of maximum follicular densities.

The SC is a primary barrier to percutaneous absorption. It is also considered the major route for various drugs or biomolecules penetration. Recent reports demonstrated that the transepidermal route, hair follicles, and sebaceous glands significantly contribute to topical or transdermal delivery. Below the skin surface, the hair follicles provide a large surface area for potential absorption of drugs or compounds, because of an enfolding of the epidermis extending deeply into the dermis.

Sebaceous glands associated with the hair follicles secrete sebum, which may in return manipulate absorption by providing a lipoidal pathway. However the detailed nature of pilosebaceous transport mechanisms has yet to be established. Recently, various studies have supported follicular drug penetration in the delivery of therapeutics, which is contradictory to previous assumptions. At the end of the 20th century, scientists working on skin delivery expressed two different opinions. One group favored the transfollicular route for drug delivery, but the other group said that the available surface area was simply too small to be of any relevance. Cosmetic scientists consider transfollicular applications for their products to be of great relevance. Therefore, the transfollicular route would be useful for effective delivery of antiacne products that are targeted to pilosebaceous units, antiperspirant products delivered to eccrine glands, or macromolecules (such as peptides and hyaluronic acid). For delivery of such product(s), the SC shows reluctance to allow penetration through the skin. With time, transfollicular delivery research became stagnant, and this led scientists to agree with the initial view of Scheuplein, who in 1967 wrote that the transfollicular pathway was limited to the early phase of skin permeation, before steady-state diffusion is accomplished. During the early 1990s, Hueber et al concluded that human skin appendages, (hair follicles and sebaceous glands) formed a penetration path for steroids and other chemical molecules of similar molecular weight and characteristics. Another approach tried to analyze the participation of the infundibulum in overall skin delivery.

Penetration of chemicals/drugs via skin of newborn (24 hours old) rats was compared with 5-day-old rat skin. In vitro penetration of hydrocortisone through skin from rats killed at 24 hours and 5 days after birth was compared. These studies showed that skin penetration was fivefold greater in the presence of intact follicular units. A less popular method of evaluating the impact of the transfollicular route on skin delivery was to test the penetration of the same compounds in like formulations through the skin of different body sites with varying hair-follicle densities, then assigning the found differences in permeation to the participation of additional hair follicles. Rolland et al reported the significance of size in transfollicular delivery of drugs and chemicals. Researchers demonstrated that polymeric microspheres (3 and 7 μm) penetrated exclusively through the transfollicular route; however, whether this was real penetration or accumulation into the pilosebaceous unit and deeper dermal tissues could not be demonstrated.

1.1 Basic structure of skin

Insight into anatomical, physiological and chemical properties of the skin is required for the knowledge of basic features of skin. Skin basically consists of four layers: 1) the SC (nonviable epidermis), 2) viable epidermis, 3) dermis, and 4) subcutaneous tissues (Figure 1). Apart from these layers, it also has numerous allied appendages: hair follicles, sweat glands, apocrine glands, and nails. The innermost layer is subcutaneous tissues, which are made up from connective fibers and fat. This layer serves as an insulator, a shock absorber, depot of calories, and supplier of required nutrients for more superficial skin layers. The base of hair follicles and secretory duct of sweat glands and cutaneous nerves, as well as networks of lymph and blood vessels, are also located in this area. The nature of the dermis is a fibrous layer

that holds up and reinforces the epidermis. Its thickness ranges from 2 to 3 mm, and is comprised of a loose connective tissue matrix that is composed of collagen (a fibrous protein, embedded in a semigel matrix that contains water, various ions, and mucopolysaccharides). This matrix facilitates the holding of cells, and allows oxygen and nutrients to diffuse into the epidermal cells. This layer has hair follicles, sebum and sweat glands, and an extensive blood supply and nerve network. The neighboring layer of the dermis is identified as the papillary layer, which offers nutritional support to the viable epidermis. The papillary layer shows an important role not only in a nutritional function but also in temperature, pressure, and pain regulation. Additionally, it contains various cells in a sparse cell population: fibroblasts, responsible for the connective tissue synthesis; mast cells, involved in the immune and inflammatory responses; and melanocytes, involved in the production of melanin. At the differentiation stage, the epidermal layers (stratum germinativum, stratum spinosum, stratum granulosum, stratum lucidum, and stratum corneum) are transformed into corneocyte cells. Here at the cellular level, changes occur, such as lamellar body extrusion, loss of the nucleus, and a rise in the keratin content until the SC is formed. The outermost layer of the epidermis is the SC, also known as the nonviable epidermis. The SC has an approximate thickness of 10–20 μm, which can differ from one body part to the other. In a given cross section of skin, it consists of 15–25 stacked, flattened, hexagonal, and cornified cells known as corneocytes or horny cells, attached to a mortar of well-arranged intercellular lipids. A brick and mortar model describes this type of arrangement of cells, which serves as a rate controlling barrier in case of transdermal absorption of drugs. Corneocytes are approximately 40 μm in diameter and 0.5 μm in width and principally comprised of insoluble bundled keratins (approximately 70%) and lipids (~20%) located in the cell covering. The intercellular matrix includes lipids and desmosomes for corneocyte cohesion.

In this area, lipids have noticeable roles in many respects:

- From the skin surface to the base of the SC, lipids constitute the continuous phase
- Among biological membranes, the composition of lipids (mainly ceramides, free fatty acids, and cholesterol) is unrivaled, and particularly the absence of phospholipid is remarkable
- Despite this shortage of phospholipids, polar bilayer-forming lipids and SC lipids present as multilamellar sheets.
- Principally saturated and long-chain hydrocarbon tails allow a highly arranged and interdigitated configuration.

In a lipid matrix, the staggered corneocyte arrangement is proposed to offer an extremely tortuous lipoidal diffusion passage: the membrane becomes 1,000-fold less permeable for water compared to other biological membranes. The intercellular lipid layer is present as a continuous phase for substances of small molecular size, thus it is referred to as the most important pathway for absorption of these kind of substances. Two to three weeks are required for complete turnover of the SC layer. It is the main barrier for exchange of substances between the body and environment, because of the composition and structure of the SC. Therefore, it is a tough task for drug delivery through the skin. Furthermore, intracutaneous metabolism, a high drainage rate because of blood and lymph capillaries appear in the dermis, and a peripheral immune system potentiate this anatomical barrier.

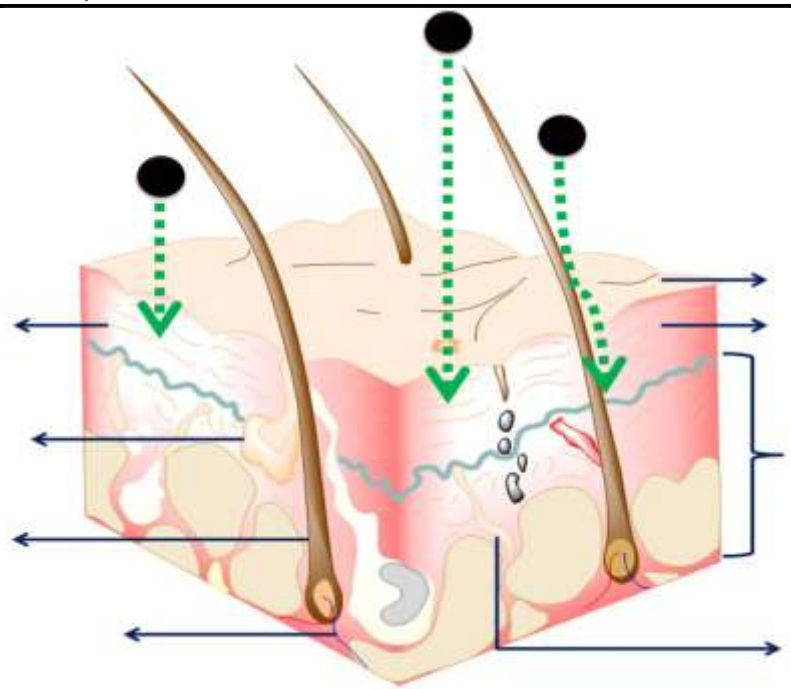

Figure 1: skin layers and possible routes of drug delivery to skin layers.

1.2 Anatomical and physiologic aspects of pilosebaceous units.

1.2.1 Hair follicles and types

Pilosebaceous units comprise an integrated organization of hair follicle, hair shaft, and adjacent arrector pili muscles with associated sebaceous glands. Hair follicles are made up of two parts: one is the hair bulb and the other is the hair shaft, which is enveloped in an inner root sheath, then an outer root sheath, and by an outermost acellular basement membrane called glassy membrane. As a keratinized layer, the outer root sheath is present throughout the epidermis, while the inner root sheath ends about halfway up to the follicle. Each hair follicle is coupled with either one or more flask-shaped sebaceous glands, which are outgrowths of epithelial cells. These holocrine glands are connected by ducts to the upper region of the follicle. Regulation of hair growth is governed by cells found near the hair bulb. Figure 1 shows various skin layers and possible routes of drug delivery to the skin strata. Human hairs are of two types: terminal and vellus. Macroscopically terminal hairs are pigmented, 2cm long, and 0.03mm thick. Terminal hairs generally contain a medullary cavity, and present more than 3mm depth into subcutaneous tissue. Another type of vellus hair is unpigmented, usually short in length (2cm), and thin (0.03mm), and these are typically distributed just 1 mm into the dermis. Interestingly, some hair follicles can exist in a transitional phase between terminal and vellus forms. The hair follicles in the scalp typically grow as a unit. Each follicular unit is composed of one to four terminal hairs and one to two vellus hairs and encircled by branches from the same arrector pili muscle. The pilosebaceous unit is a complex and dynamically three-dimensional (3D) structure that controls various activities of a biochemical, immunological, and metabolic nature.

1.2.2 Hair cycle

Hair follicles have a specific growth cycle that includes alternating multiplication and rest phases. Hair follicles show a growth cycle of three major phases:

- Anagen or growth phase – rapid proliferation occurs in a continuous manner to make the inner root sheath, and moves in an upward direction to form the hair shaft
- Catagen or involution phase – in this phase, three processes occur: end of mitosis, reabsorption, and cell death of the lower follicle segment
- Telogen or resting phase – prior to the hair being shed. In recent times, the two other stages – exogen (release of telogen fibers from hair follicles) and kenogen (lag time between exogen and development of new anagen fiber) – have been expressed as the hair-growth phase. More than 85% of scalp follicles are found in the anagen phase (period 2–6 years), while approximately 2% of

scalp follicles follow the catagen phase (2 weeks), and approximately 10% are in the telogen phase (2–4 months). The elongation rate of the scalp-hair shaft has been found to be 0.3–0.4 mm per day. Proliferation and subsequent differentiation of the matrix keratinocytes in bulb sites affect the rate of elongation of hair shafts. The size of the hair bulb determines the thickness of the hair shaft. If changes occur in the hair cycle, this results in the majority of hair-growth problems. Androgenetic alopecia is caused by a shortening of the anagen stage, with a clinical consequence of more hair loss, followed by a conversion of terminal to vellus hair follicles, termed miniaturization. However, hypertrichosis and hirsutism conditions can show a prolonged anagen phase with conversion of vellus hair follicles into terminal. The endocrine system, and particularly the pineal gland, modulates hair growth upon seasonal changes, because of a reciprocal relationship between circulating prolactin levels and melatonin concentrations, elevated during summer and lessened in winter.

The synthesis and release of sebum are additional key functions of pilosebaceous units, comprised of short-chain fatty acids with fungistatic and bacteriostatic properties. The total disintegration of glandular cells of pilosebaceous units secretes sebum and is discharged through ducts into the upper third of the follicular canal. In this region of the follicle, sebum provides an environment of neutral and nonpolar lipids. The human sebum contains 57% triglycerides, 26% wax esters, and approximately 2% squalene. Sex hormones and age affect glandular activity for secretion of sebum. Secretion is lacking in infants, accelerated at puberty, and decreased in elderly persons. Interestingly, the density or size of follicles is not affected by the sebum-production rate, but there is some contention related to the effect of temperature on the secretion of sebum. It has been found that secretion is steady irrespective of season, but other evidence suggests that sebum output is augmented in hot conditions.

1.2.3 Types of hair follicles

Generally, hair follicles are of two types: terminal follicles which are androgen-free hair (eyebrows, lashes) and vellus follicles which are hormone-dependent hair on the scalp, beard, chest, axillae, and pubic region. They are comprised of 0.2 cm long terminal hair shafts with a thickness of 0.60 mm, are pigmented, and contain medullae. Most scalp hairs are not medullated, and medullae are only present in prominent terminal hair fibers. Terminal hair generally extends more than 3 mm into the hypodermis. The remaining body of adults is covered with vellus hair, short (2 cm) and thin (30 mm diameter). These hairs are usually unpigmented and extend just 1 mm into the dermis part. Some hair follicles can exist in a transitional phase between terminal and vellus forms. Palms of the hand, soles of the feet, lips, and parts of the external genitalia are only the skin regions devoid of hair follicles. The hair follicles in the scalp region are characteristically organized in the follicular unit, comprised of one to four terminal hairs and one to two vellus hairs, and encircled by branches of arrector pili muscle.

1.3 Numeric occurrence and size of hair follicles

In the past, follicular penetration was ignored, because it was assumed that hair follicles covered 0.1% of total skin area. However, recent studies have concluded that the above assumption is acceptable for the inner side of the forearm, which is generally employed for skin-permeation studies as an experimental region. However, hair follicles of different body regions show variations in number of hair follicles, follicular orifice size, diameter of hair shafts, and volume and surface of infundibula. For follicular penetration studies, knowledge of hair-follicle density and size are a necessary requirement. Hair shafts show comparatively minute differences in diameter (16–42 mm). Maximum shaft diameters are observed in the sural (42 mm) and thigh (29 mm) regions, with the narrowest on the forehead (16 mm). The maximum hair-follicle density is found on the forehead, ie, 292 follicles/cm2 . The maximum follicular infundibula volume, which is represented as a potential follicular reservoir for dermally enforced compounds, is found on the forehead, ie, 0.19 mm3 /cm2, as well as in the sural area, ie, 0.18 mm3 /cm2 . In comparison to the reservoir of the SC, all follicles are open for the penetration process in the follicular reservoir on the forehead. For the scalp and face, the combined areas of follicular openings can be more than 10% of the total skin area.

1.4 Transfollicular drug delivery

1.4.1 Hair follicles and potential drug-targeting sites

The medulla, cortex with melanosomes, and the cuticula constitute the hair shaft, and have flat and cornified cells (roof-tile arrangement). The hair shaft can be divided into:

- The infundibulum, present between the skin surface and the duct-opening point of the sebaceous gland to the hair canal
- The isthmus, found between the bulge area and the duct-opening point of the sebaceous gland
- The suprabulbar zone, where differentiation of different layers of anagen follicles start and are identified very easily at this level
- The hair bulb, with the dermal papillae linked to the blood vessels.

The outer root sheath is a stratified epithelium that surrounds the hair follicle continuously with the epidermis. The superficial portion of the hair-follicle infundibulum (acroinfundibulum) is lined by the epidermis, including a considerably developed SC and a stratum granulosum layer. The lower region of the infundibulum, referred to as the infrainfundibulum, may get an uninterrupted loss of epidermal differentiation toward the isthmus, and acts as a most important entry portal for applied contents.

The sebaceous gland serves as a potential therapeutic target site, and is engaged in acne etiology and androgenic alopecia. 5α-Reductase is expressed in androgenic alopecia, particularly in regions of the face and scalp, and changes testosterone to the more potent metabolite 5α-dihydrotestosterone. Considerable efforts have been reported to show the maximum accumulation of different bimolecular substances in androgen-dependent glands. Additionally, a wide capillary bed coupled with the upper dermal vasculature provides the upper follicle and sebaceous glands with blood, producing the opportunity of systemic drug delivery. The bulge region is situated just below the sebaceous glands, which is responsible for follicle reconstitution and could be another attractive targeting site. It is comprised of stem cells of high proliferative capacity. These cellular areas are the specific target area for gene delivery to help in long-term correction of genes in cases of genetic skin disorders/congenital hair disorders. The hair-bulb region with hair-matrix cells regulates hair growth and pigmentation.

Teichmann et al developed a method to differentiate transepidermal and transfollicular permeation. They utilized a varnish–wax mixture to block follicles selectively. The varnish–wax mixture was used for the determination of chemical and physical ultraviolet filters and curcumin penetration into follicles, in addition to in vivo follicular penetration of caffeine, which was utilized in a shampoo formulation. Differential stripping allows determination of the amount of a topically applied substance that penetrates into the hair follicles. The technique combines the tape-stripping procedure (removing the SC layer by layer), followed by biopsies of cyanoacrylate skin surface (taking out the components of the follicular infundibulum, the "follicular cast" consisting of a mixture of keratinized material, cell detritus, lipids and, bacteria).

1.5 Physical methods for Topical Drug Delivery

Different strategies for drug penetration enhancement can be used aiming to circumvent the SC barrier. Among them, occlusion, formulation optimization and physical methods can be used alone or combined. Physical methods can potentially increase the transport of macromolecules to the SC, enabling higher concentrations of drugs into deep skin layers. Thus, much effort has been conducted aiming for the transdermal drug delivery using physical methods. The most studied are iontophoresis, sonophoresis and microneedles. In the following subsections, these methods concepts and mechanisms will be presented. Recent research related to these methods for topical action will be discussed in the next section.

1.5.1 Iontophoresis

Iontophoresis consists on the application of low intensity electric current, usually up to 0.5 mA/cm², on biological membranes or tissues, such as the skin, to deliver therapeutic molecules aiming for topical or transdermal effect. The total iontophoretic flux of the drug refers to the sum of electromigration and electroosmosis contributions. Basically, the relative importance of each of these transport mechanisms is related to the physicochemical and electrical characteristics of the skin and the drug. Briefly, an electric field is applied across the skin and distributed with the help of two electrodes, a positive one, the anode, and a negative one, the cathode (Figure 1). Preferably, an ionized drug is placed in a compartment in contact with the electrode of equal polarity. Thus, cationic drugs are placed in the anode compartment, whereas anionic ones are placed in the cathode. This is usually made because the application of an electric current in the skin results in

cations migration toward the cathode and in anions migration in the opposite direction. This facilitated migration of ionized substances increases drugs transport through the skin.

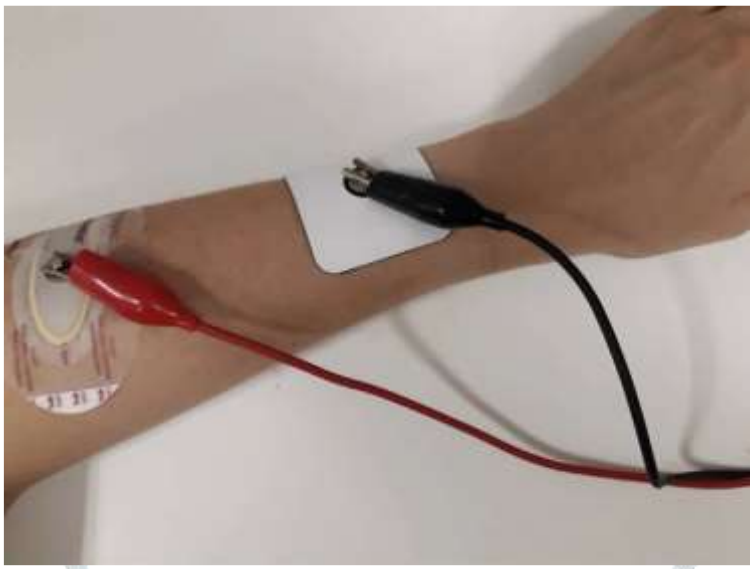

Figure 2: Experimental setup for in vitro iontophoresis using Logel

1.5.2 Sonophoresis

Sonophoresis, also named ultrasound or phonophoresis refers to the transport of drugs into and through the skin during or after the application of ultrasound. Ultrasonic waves are generated by an electric signal, which is amplified and sent to the horn of an ultrasonic transducer. When the electric signal reaches the horn, it is converted into a mechanical wave by piezoelectric crystals, located at the tip of the transducer, and is transmitted to a coupling medium. In topical application, the coupling medium is placed on the skin (Figure 2). The amplitude and the frequency with which the ultrasound is applied influence the oscillation of sound waves, resulting in the formation of different areas of rarefaction (low pressure) and compression (high pressure) in the medium, which cause different changes in skin permeability. Thus, amplitude and frequency are important parameters, where the amplitude refers to the ultrasound horn displacement during each half cycle and the frequency is related to the number of times that the tip is moved per second [58]. Ultrasound frequencies can range from 20 kHz to 16 MHz, but usually low (20-200 kHz) and medium ultrasound (0.2-1 MHz) frequencies, which possess high cavitational effects, are applied for drug delivery in the skin. Cavitation is considered the main mechanism responsible for increased skin permeability, especially when using low frequency ultrasound. Cavitation can be defined as the process by which air bubbles or cavities are formed in a medium in response to pressure variation caused by the movement of the sound wave. As shown in equation II, the radius of these bubbles is inversely proportional to the frequency of application of the ultrasound (Equation II). Equation II where: r corresponds to the resonant radius of the cavitation bubble, f corresponds to the ultrasound frequency and C corresponds to a constant that is related to the properties of the coupling medium.

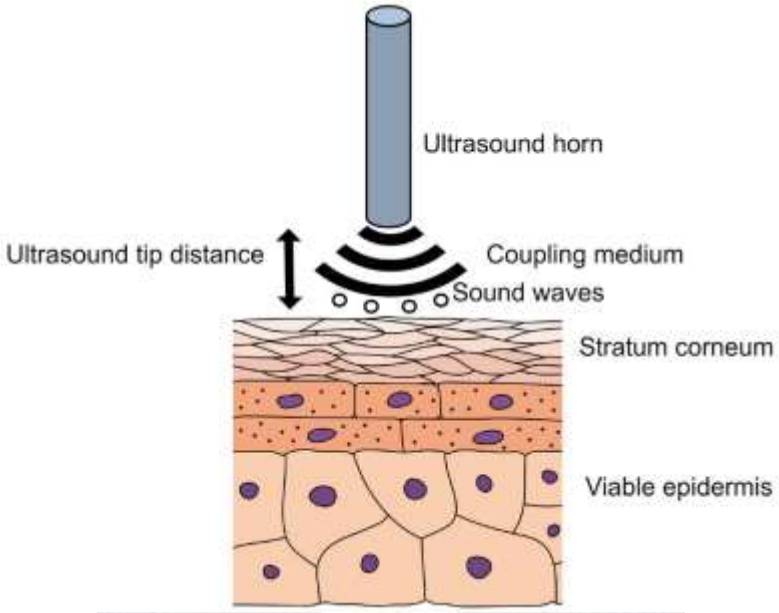

Figure 3: Schematic representation of low frequency ultrasound application on skin surface

1.6 Amphiphiles

Self-assembly processes involving amphiphilic macromolecules provide unique and new opportunities for designing novel materials for advanced application in nanotechnology. The thermodynamic incompatibility between the different blocks causes a spatial organization into ordered morphologies on the nanoscale with the production of novel structural features, as demonstrated by recent studies. Leading examples can be found in biosystems where assemblies of different amphiphilic macromolecular components and their integrated actions allow the performance of highly specific cellular functions. In the first part of this review we present a tutorial introduction to the basic aspect of traditional, head/tail(s) type, amphiphiles whose aggregation is driven by soft interactions such as hydrogen bonds and steric effects and hydrophobic and electrostatic interaction. Moreover, we highlight important examples where complex processes such as the structure modulation and control of morphology by other structure directing interactions can stimulate advanced application in materials science as well as in biological and medicinal chemistry. Finally, we provide insight into the novel structural features obtained by the precise tailoring of chemical structures and the efficient use of noncovalent forces for the introduction of chirality, signal processing, and recognition processes. The reversibility of noncovalent interactions allows dynamic switching of nanostructures morphology and functions in response to various external stimuli which further provides a flexible platform for the design and fabrication of smart amphiphilic nanomaterials and functional supramolecular devices.

1.6.1 Characteristic and Basic Properties of Amphiphiles

Amphiphiles are compounds possessing both hydrophilic (water-loving) and lipophilic (fat-loving) or water-hating components. In conventional head/tail(s) amphiphiles the lipophilic part consists generally of a long (saturated or unsaturated) hydrocarbon chain, while the hydrophilic head can be either nonionic or ionic. Nonionic surfactants have either polyether or polyhydroxyl units as the hydrophilic group. A large variety of conventional nonionic surfactants consist generally of a hydrophilic poly(ethylene oxide) chain, often called ethoxylates, connected with a hydrophobic alkyl chain, and are generally used in cleaning applications with anionic surfactants. For example, polyoxyethylene alkyl ethers, are nonionic surfactants made of hydrophilic oxyethylene units and an alkyl chain with methylene groups (Figure 1(a)). Anionic surfactants, which are widely used as detergents and soap for cleaning processes, consist generally of negatively charged headgroups and positively charged counterions (such as sodium, potassium, or ammonium ions). Carboxylate, sulfate, sulphonate, and phosphate are the commonly used polar groups (Figure 1(b)). Cationic surfactants consist of positively charged headgroups such as a quaternary ammonium and a halide ion as a counterion. Cetyltrimethylammonium bromide (CTAB) and sodium bis(2-ethylhexyl) sulfosuccinate (AOT) are the most employed cationic amphiphiles (Figures 1(b) and 1(c)). Finally in zwitterionic amphiphiles the headgroups possess both a positive and negative charge, as it happens, for example, in the vesicle-forming phospholipid

phosphatidylcholine. For example, if zwitterions contain a carboxylate and a protonated ammonium ion, it may behave as an anion (at high pH) or a cation (at low pH) assuming then an amphoteric character. Some traditional amphiphilic molecules are reported in Figure 4.

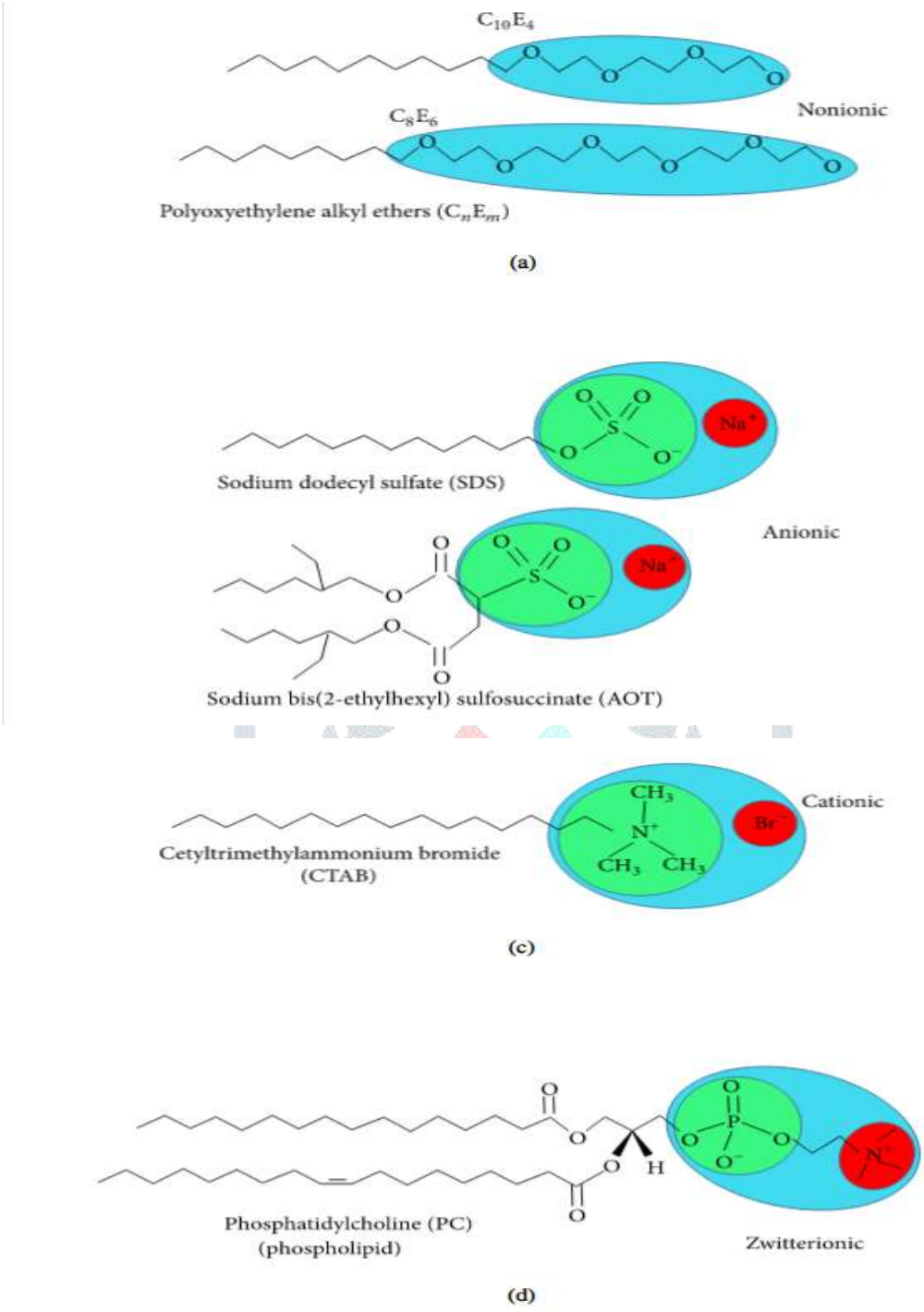

Figure 4: Example of most common nonionic (a), anionic (b), cationic (c), and zwitterionic (d) amphiphilic molecule

Due to their amphiphilicity (or surface activity), the amphiphiles polar headgroup interacts with the water while the nonpolar lipophilic chain will migrate above the interface (either in the air or in a nonpolar liquid). In this case the disruption of the cohesive energy at the interface favors a microphase separation between the selective solvent and the dispersed phase of the amphiphile with the formation of many smaller closed interfaces or micelles-like aggregates. Due to their ability to reduce the interfacial tension amphiphilic molecules are often called surfactants (i.e., surface active agents). For this reason amphiphiles play an important role as emulsifiers, detergents, dispersants, and wetting and foaming agents in several applications.

1.7 Self-Assembly of Amphiphilic Compounds

Self-assembling systems based on amphiphilic compounds find wide application in different fundamental and practical areas due to their unique ability to form nanoscale assemblies with gradients of polarity, viscosity, electric charge and other characteristics. In an aqueous medium, such nanosized aggregates possess a nonpolar interior capable of entrapping guest molecules, thereby dramatically changing their properties. This phenomenon is responsible for the wide range of applications of amphiphilic compounds in cosmetics, food industry, pharmacy, drug and gene delivery, etc. Meanwhile, for these reasons they are strongly required to meet the green chemistry criteria. Therefore, the design of environmentally friendly amphiphilic compound (surfactants, macrocycles, polymers) is a challenging task from the viewpoint of the development of supramolecular multifunctional systems with tunable characteristics.

1.7.1 Cationic Surfactants Bearing Cleavable Fragments

Among amphiphilic compounds, special attention is received by cationic surfactants, which is related to both their fundamental and practical relevance. Researchers have succeeded in designing and synthesizing a variety of homologous series of cationic surfactants differing in the structure of head groups, which allows for determining the role of the polar fragment in the physicochemical properties and functional activity of supramolecular systems based on cationic surfactants in terms of structure–properties–activity relationships. Numerous fundamental approaches and practical applications involving cationic surfactants have recently been demonstrated in the fields of biochemistry, nanomedicine, pharmacy, catalysis, corrosion protection, oil recovery, food, cosmetics, etc. These beneficial results were achieved despite the well-known toxicity of cationic surfactants, since much effort has been undertaken to overcome this limitation. Therefore, the design of novel cationic surfactants addressing this problem is of importance. To this end: (i) cationic surfactants with specific structures, including cleavable, gemini, and biocompatible surfactants have been designed; (ii) mixed compositions with less toxic nonionic surfactants are used; (iii) modifications with hydrotropic agents are carried out. Some of these studies devoted to synthesis and use of novel amphiphilic compounds answering biotechnological criteria are discussed below, with emphasis on cationic surfactants. Recently, much attention has been received by the so-called cleavable surfactants bearing ester, amide, disulfide or other degradable fragments. While researchers initially focused on ester quats bearing quaternized nitrogens in the polar group, more diverse amphiphilic structures have been designed, including those containing a carbamate moiety, gemini analogs, or amphiphilic matrices bearing two cleavable groups. The structural characteristics of ester quats are of importance in their surface activity, with synergetic hydrolysis-driven effects being observed for derivatives in which the carbonyl groups are bridged by an oxygen atom with a quarternized nitrogen atom. Series of gemini surfactants bearing ester and amide groups were synthesized and systematically studied in, with exploration of their degradability, surface activity, foaming and antimicrobial properties.

1.8 Amphiphilic Compounds with Natural Fragment

Among the wide spectrum of recently synthesized amphiphilic compounds a special place is occupied by amphiphiles bearing natural fragments in their structures. The main idea behind the design of this type of amphiphilic compounds is based on principles of biomimetics that allow constructing environmentally and physiologically friendly supramolecular systems of nanoscale dimensions for a number of practical applications in industry and biomedicine.

1.8.1 Amphiphilic Compounds Bearing Amino Acid Fragments

One of the most popular routes for modification of amphiphilic compounds and making systems on their basis more biocompatible and bioavailable is the introduction of amino acid fragments into their chemical structures. These synthetic amino acid-based surfactants are an alternative to ordinary antimicrobial compounds, because they can be obtained from renewable raw materials.

Amino acid-based amphiphiles are promising in obtaining drugs based on surfactant–protein complexes and can be used in oil recovery, as nonviral vectors in gene therapy, in cosmetics, etc. The main requirements for the resulting amphiphiles are multifunctionality, low toxicity and biodegradability.

It is well known that in accordance with one of the conventional classifications of amino acids from the viewpoint of their charge characteristics provided by the nature of their substituents, they could be divided into four big groups [87]: (1) nonpolar amino acids; (2) polar amino acids; (3) polar acidic amino acids (negatively charged); (4) polar basic amino acids (positively charged). Since the charge of an amphiphilic compound determines its properties to a great extent, the corresponding derivatives of amino acids should be discussed from this perspective.

1.8.2 Sugar-Based Amphiphilic Compounds

Another promising approach to design substances meeting biomedical application criteria is the functionalization of amphiphiles by a saccharide moiety that makes it possible to prepare sugar-based surfactants, such as alkylpolyglycosides, alkylglucamines, etc. Among the obvious advantages of these substances are their biodegradability, low toxicity and low cost. This research direction looks so promising, that researchers have used significant theoretical approaches to predict their aggregation parameters. An overview of the reports dedicated to sugar-containing amphiphiles allows one to deduce that these compounds could be classified by two ways from the viewpoint of the degree of oligomerization of the sugar moiety inserted in the chemical structure of an amphiphilic compound. The first classification takes into account the number of furanose and/or pyranose moieties in the structure and therefore the compounds can be divided into three groups: (1) amphiphiles bearing monosaccharide fragments; (2) amphiphilic compounds containing disaccharide moieties; (3) hydrophobized derivatives of trisaccharides. Another classification is based on the nature of the head group and the number of hydrophobic tails and head groups of amphiphiles, so these derivatives could be divided into: (i) monomeric nonionic surfactants, (ii) nonionic gemini surfactants and (iii) cationic surfactants and other amphiphiles with a sugar fragment. Herein, we consider some general properties for each of the six mentioned groups.

2.0. Experimental Work

2.1. Materials and Equipment's

Table 2.1: List of Instruments

S. No.	Instruments	Manufacturer
1	UV/VIS Spectrophotometer,	Shimadzu, Japan
2	Digital Weighing balance, (CY220)	Shimadzu, Japan
3	Viscometer	Anton Paar, Austria
4	Ultra sonicator	PCi analytics, India
5	Vortex mixer	Remi Scientific Instruments, Mumbai
6	Hot air oven	P. L. Tandon& Co, Delhi
7	Particle Size	Anton Paar, Austria
8	pH Meter	Ohaus, USA
9	Melting Point Apparatus	Remi Scientific Instruments, Mumbai
10	Infrared red spectrophotometer (FTIR)	Bruker Alpha, Berlin, Germany
11	Microcentrifuge	Remi Scientific Instruments, Mumbai
12	Vacuum pump	Suguna single phase, Chennai, India

Table 2.2: List of Chemicals

S. No	Materials	Source
1	Ciclopirox Olamine	Global Pharma, Mumbai
2	Potassium Dihydrogen orthophosphate	Signet Chemical Corp. Pvt. Ltd., Mumbai
3	Disodium hydrogen orthophosphate	Central Drug House Pvt. Ltd. New Delhi
4	Ethanol	Changshu Yanguan Chemical, China
5	Methanol	Fisher Chemical Ltd., Ahmedabad
6	Iso propyl alcohol	Fisher Scientific India Pvt. Ltd.
7	HCl	SD Fine-chem. Ltd, Mumbai
8	n-octanol	SD Fine-chem. Ltd, Mumbai
9	Sodium Hydroxide	Fisher Chemical Ltd., Ahmedabad
10	Calcium chloride	SD Fine-chem. Ltd, Mumbai

2.2. Pre-formulation studies

An essential step in the overall development process is pre-formulation. Prior to compounding, it is the study of the physical and chemical characteristics of the medicine. These investigations concentrate on the physicochemical characteristics of the medicine that may have an impact on its effectiveness and the creation of an effective dosage form. A detailed comprehension of these characteristics might ultimately justify formulation design or highlight the necessity of molecular change. These pre-formulation studies could, in the simplest scenario, just confirm that there aren't any major obstacles to the compound's development. These investigations are a necessary part of the development process for a stable, reliable dosage form. By using several analytical methods, including IR spectroscopy, UV spectroscopy, melting point, etc., the acquired drug sample was identified.

2.2.1. Organoleptic Characteristics:

The drug sample was characterized for the physical characterization like appearance, color and odor.

2.2.2. Melting point

For determination of melting point USP method was followed. Small quantity of Ciclopirox was placed into a sealed capillary tube. The tube was placed in the melting point apparatus. The temperature in the apparatus was gradually increased and the observation of temperature was noted at which Ciclopirox started to melt and the temperature when the entire drug gets melted. This method is also known as capillary method.

2.2.3. UV spectrum of Ciclopirox in Methanol

When exposed to light in the visible or ultraviolet regions of the spectrum, molecules in solution absorb light of a certain wavelength based on the type of electronic transition associated with the absorption. This information is often obtained using a UV-visible spectrophotometer. In most cases, the UV spectrum is represented as a plot of absorbance vs wavelength**.** To determine the maximum amount of medication, a double beam UV-visible spectrophotometer was utilised. The range of 200-400 nm was used to scan at a concentration of 100µg/ml in methanol.

2.2.4. Estimation of Ciclopirox

2.2.4.2. Estimation of Ciclopirox by UV-visible spectrophotometer in methanol

Ciclopirox normal stock solution 10mg in 100ml (100ppm) was made in methanol and methanol was used to dilute this solution, yielding varied concentrations ranging from 5 to 35µg/ml in UV-visible spectrophotometer. The absorbance of these solutions was measured at 301 nm with methanol serving as the blank, and a standard curve was drawn against concentration. Intercept, slope, straight line equation, and correlation coefficient were calculated from the calibration curve.

2.2.5. Partition Coefficient of Drug

Indicators of a drug's lipophilicity and hydrophilicity, as well as its capacity to cross cell membranes, include partition coefficient (oil/water). The ratio of unionised medication dispersed between the organic and aqueous phases at equilibrium is what is meant by this term. A way to describe the drug's lipophilic/hydrophilic characteristics is by partition coefficient. Drugs with P values significantly over 1 are considered lipophilic, whereas those with P values significantly below 1 are considered hydrophilic. Typically, an oil phase of n-octanol and water is used to calculate the partition coefficient. When n-octanol and water are involved:

$P_{o/w} = C_{n\text{-}octanol}/C_{water}$

The partition coefficient ($P_{o/w}$) therefore is the quotient of two concentrations of drug in n-octanol ($C_{n\text{-}octanol}$) and water (C_{water}) respectively and is usually given in the form of its logarithm to base 10 (log P).

- Shake flask method

The shake flask method was used to carry out the investigation on partition coefficient determination. Ciclopirox was dissolved in excess amounts in 3 ml of n-octanol and water (1:1) and left for 24 hours. The two layers were divided after 24 hours and centrifuged for 15 min. at 15,000 rpm. After the proper dilution, the absorbance was measured in a UV spectrophotometer.

2.2.6. Solubility Study

Solubility is the spontaneous interaction of two or more compounds to produce a uniform molecular dispersion.

For the quantitative solubility investigation, excess amounts of the medication were placed in culture tubes that had been carefully cleaned and contained 1ml of each of the following solvents: water, phosphate buffer saline pH 7.4, ethanol, methanol. These culture tubes were shaken for 24 hours at room temperature on a water bath shaker. Each sample was centrifuged at 15,000 rpm after 24 hours, and the supernatant was removed. The filtrates were then appropriately diluted and the supernatant was filtered before being measured spectrophotometrically.

2.2.7. FTIR of Ciclopirox and Excipients

The FT-IR (Fourier Transform Infrared) spectra of a substance or medication can reveal the groups that are present. For structure investigation, FT-IR spectroscopy was employed. For the purpose of identifying any potential medication interactions with excipients, an FT-IR spectrum of a mixture of Ciclopirox and other ingredients was recorded.The FT-IR chamber received 1-2 mg ofCiclopirox. The region between 4000 and 400 cm-1 of the infrared spectrum was observed.

FT-IR was used to determine whether the medicine and excipients were compatible. FTIR was employed as a method to look for any chemical or physical interactions between the excipients and the medication. Drug and other excipients were fully combined in a 1:1 ratio. Samples were FTIR scanned between 400 and 4000 cm-1. To assess for incompatibility and physical changes, the spectra of drugs in their pure and excipient forms were compared.

2.3 Preparation of micellar nanocarrier of Ciclopirox olamine

2.3.1 Thin film hydration method

Ciclopirox olamine Nanocarrier micellar were prepared using by thin film hydration technique method with modification. Briefly, Ciclopirox olamine equivalent to dose, different Molar ratio of Phosphatidylcholine (5 to 15M) and Pluronic (0.5 to 2.5 M) were accurately

weighed and dissolved in chloroform: methanol (7:3) in a round-bottom 250mL flask. The solvent was slowly evaporated at 60ºC under reduced pressure using a rotary evaporator, revolving at 120 rpm for 1 h until a thin dry film was formed on the inner wall of the flask. The dried film was treated with distilled water and the flask was allowed to revolve at a fixed hydration temperature of 60ºC for 30 min under normal pressure. The mixture was then sonicated for 1 min and the volume was adjusted into 10mL at room temperature (25 ºC) to obtain nanocarrier dispersions.

2.3.1.1 Probe sonication process: In order to reduce the dimensions of the micelles for targeting delivery, a probe sonication for 5 min in a pulsatile manner (50 s sonication with 10 s pause) with 30% amplitude.

Table No. 2.3: Composition of Ciclopirox olamine-loaded polymeric micelles

Experimental trial no.	PC: Pluronic molar Ratio	Drug (%w/v)	Phospholipids E80 (%w/v)	Pluronic F127 (%w/v)
F1	5:1	1	0.39	1.26
F2	10:1	1	0.78	1.26
F3	15:1	1	1.17	1.26
F4	10:0.5	1	0.78	0.63
F5	10:1.5	1	0.78	1.89
F6	10:2.0	1	0.78	2.52
F7	10:2.5	1	0.78	3.15

1.3.2 Evaluation of polymeric micelles formulation

1.3.2.1 Visual Appearance: Micellar nanocarrier dispersion was examined by visual inspection to verify sample homogeneity, phase separation and presence for aggregates.

1.3.2.2 Determination of percentage Entrapment efficiency

The entrapment efficiency of micelles was determined by calculating the amount of unentrapped drug in the micelles. A defined amount of micelles dispersion was transferred in centrifuge tube. The dispersion was centrifuge for 30 min at 18000 rpm. After centrifugation the supernatant was collected followed diluted methanol and percentage drug entrapment was determined using spectrophotometer. The entrapment efficiency has been determined according to the following equation:

$$EE\ \% = \frac{W_{(Added\ drug)} - W_{(free\ drug)}}{W_{(Added\ drug)}} \times 100$$

Where, W (added drug) is the amount of drug added during the preparation, W (free drug) is the amount of free drug measured into supernatant after centrifugation.

1.3.2.3 Particle Size & zeta potential: Particle size and polydispersity index of dispersion were measured by a dynamic light scattering process. Vesicle properties, particle size diameter were determined at room temperature. For the particle size measurements, the dispersion was suitably diluted with distilled water in order to avoid multiscattering phenomena.

1.3.2.4 TEM

The morphologic examination of the selected formulations was performed by transmission electron microscopy (TEM) operating at 80 kV. One drop of the diluted dispersion was deposited on the surface of a carbon coated copper grid, negatively stained with 2% phosphotungstic acid then allowed to dry at room temperature for 10 min for investigation by TEM.

3.4 Preparation of Ciclopirox olamine-loaded polymeric micelles shampoos

The formulation batches were conducted in order to find an optimal shampoo formulation. The quantities of SLS, lanolin, sodium EDTA, Tween 80, urea, salicylic acid, and xanthan gum as given in Table 5.4. The shampoo formulations were prepared by mixing the ingredients in micelles dispersion using a magnetic stirrer operating at 500rpm. The final pH of the shampoo was adjusted between 5-6 either by 0.4N NaOH solution.

Table No. 2.4: Composition of Ciclopirox olamine-loaded polymeric micelles shampoos

Sr. No	Ingredients	Formulation Code	
		F8	F9
1	Ciclopirox olamine-loaded micelles Dispersion (ml)	100	100
2	Sodium lauryl sulphate (SLS)	15	15
3	Lanolin	1	1
4	Sodium EDTA	0.25	0.25
5	Xanthan gum	2	3
6	Tween 80	1	1
7	Urea	1.5	1.5
8	Salicylic acid	0.5	0.5
9	Sodium Hydroxide	q.s	q.s

3.4.1 Evaluation of Ciclopirox olamine-loaded polymeric micelles shampoos

3.4.1.1 Organoleptic Properties

The prepared anti-dandruff shampoos were compared with the marketed anti-dandruff shampoos based on sensory evaluation. The shampoos were inspected for color, clarity, odor, andtexture.

3.4.1.2 Determination of pH

The pH meter was calibrated using standard buffer solution such as pH 4, 7 and 9. About The pH values of prepared shampoos was determined using a digital pH meter at ambient temperature 25 ± 0.2°C. pH was measured in triplicate and average values were calculated.

3.4.1.3 Viscosity

The sample was placed in a beaker and was allowed to equilibrate for 5 min before measuring the dial reading using a T-4 spindle at 5 rpm. At the speed, the corresponding dial reading on the viscometer was noted. The spindle speed was successively lowered and the corresponding dial reading was noted. The measurements were carried in triplicate.

3.4.1.4 Solid content determination

The percentage of solid contents was measured by the loss-on-drying method. Briefly, 5 g of each shampoo formulation was poured in clean, dry, and pre-weighed Petri dishes, and the final weight was recorded. This was followed by placing Petri dishes in a convection oven set at 50°C for 1 h or until shampoos were completely dried. The dried Petri dishes were weighed again, and the solid content after drying was estimated using the following formula:

Solid contents (%)=$\frac{Wo-W1}{Wo}$x100

Where, Wo is the initial weight of the sample while W1 is the weight of solid contents.

3.4.1.5 Foam Volume

Cylinder shake method was used for determining foaming ability. 50ml of the 1% shampoo solution was put into a 250 ml graduated cylinder and covered the cylinder with hand and shaken for 10times. The total volumes of the foam contents after 1 minute shaking were recorded. The foam volume was calculated only. Immediately after shaking the volume of foam at 1 minute intervals for 4 minutes were recorded.

3.4.1.6 Dirt Dispersion

Two drops of shampoo were added to 10 mL of distilled water in a test tube, followed by the addition of one drop of Indian ink. The test tube was stoppered and gently shaken10 times. The amount of Indian ink was visually estimated in the foam as none, light, moderate and heavy. Shampoos that caused the color to stay in the foam were considered low quality.

3.4.1.7 Wetting Dispersion

The wetting time of shampoos was determined by dropping 50 mL of 1% aqueous shampoo solution on 1g of wool yarn in a 100 mL beaker. The time when wool yarn started to float at the surface of the shampoo solution and when it started to sink was recorded carefully by a stopwatch. The mean values and standard error of at least three replicates were reported.

3.4.1.8 FTIR Spectra of final formulation

FTIR spectrophotometer was used for infrared spectroscopy, and the spectrum was acquired in the (4000 - 400 cm-1) wavelength range. The process involved distributing the sample using an optimised formula.

3.4.1.9 In vitro drug release studies

Franz diffusion cell was used to determine the release profile of drug from Ciclopirox olamine loaded micells based shampoos. The cells consisted of donor and receptor chambers between which a cellophane diffusion membrane. Capacity of receptor chamber was 18ml. A magnetic bead was placed in the receptor chamber. The diffusion medium consisted of phosphate buffer saline (PBS) pH 7.4. Whole assembly was put on magnetic stirrer at 100rpm stirring speed and temperature was maintained 37.0 ± 0.5C. The 1ml samples equivalent to 1mg drug were kept over the membrane in donor compartment and stirred. 1ml samples were withdrawn from the receptor compartment at predetermined time intervals, and the volume was replenished with same volume of diffusion medium. Addition of diffusion medium to the receptor compartment was performed with great care to avoid trapping air beneath the diffusion membrane. The samples were analyzed spectrophotometrically after appropriate dilutions. The % drug release was calculated and graph of % drug release vs time was plotted. For each formulation, the release studies were performed in triplicate.

3.4.1.10 Drug release kinetic studies

Model dependent methods are based on different mathematical functions, which describe the release profile. Once a suitable function has been selected, the release profiles are evaluated depending on the derived model parameters. The data obtained from ex vivo permeation studies were plotted in different models of data treatment as follows;

- Zero Order model
- First Order model
- Higuchi's Model
- Korsmeyer-Peppas model

3.4.1.10.1 Zero order kinetics

It can be used to describe the drug dissolution of several types of modified release pharmaceutical dosage forms, as in the case of some transdermal systems, as well as matrix tablets with low soluble drugs in coated forms, osmotic systems, etc. In its simplest form, zero order release can be represented as:

$Q_0 - Q_t = K_0 t$

Where, Q_t is the amount of drug dissolved in time t, Q_0 is the initial amount of drug in the solution (most times, $Q_0 = 0$) and K_0 is the zero order release constant expressed in units of concentration/time. To study the release kinetics, data obtained from in vitro drug permeation studies were plotted as cumulative amount of drug released versus time.

3.4.1.10.2 First order kinetics

It can be used to describe the drug dissolution in pharmaceutical dosage forms such as those containing water-soluble drugs in porous matrices. The release of the drug which followed first order kinetics can be expressed by the equation:

$\log C = \log C_0 - K.t / 2.303$

Where, C0 is the initial concentration of drug, k is the first order rate constant, and t is the time. The data obtained are plotted as log cumulative percentage of drug remaining vs. time which would yield a straight line with a slope of K/2.303.

3.4.1.10.3 Higuchi's Model

This model expected to pronounce drug release from a matrix system. Primarily regarded for planar systems, it was then extended to different geometrics and porous systems. This model is based on the hypotheses that (i) initial drug concentration in the matrix is much higher than drug solubility; (ii) drug diffusion takes place only in one dimension (edge effect must be negligible), (iii) drug particles are much smaller than system thickness, (iv) matrix swelling and dissolution are negligible, (v) drug diffusivity is constant, and (vi) perfect sink conditions are always attained in the release environment.

Higuchi was the first to derive an equation to describe the release of a drug from an insoluble matrix as the square root of a time-dependent process based on Fickian diffusion. Simplified Higuchi equation is following;

$Q_t = K_H (t)^{0.5}$

Where, Qt is the amount of drug released in time t and K_H is the release rate constant for the Higuchi model. When the data is plotted as cumulative drug released versus square root of time, it yields a straight line, indicating that the drug was released by diffusion mechanism. The slope is equal to 'K_H'.

3.4.1.10.4 Korsmeyer-Peppas Model

Korsmeyer derived a simple relationship which described drug release from a polymeric system.

The release rates from controlled release polymeric matrices can be described by the equation proposed by Korsmeyeret al.

$Q = K.t^n$

Where, Q is the percentage of drug released at time't' K is a kinetic constant incorporating structural and geometric characteristics of the tablets and 'n' is the diffusional exponent indicative of the release mechanism.

For Fickian release, n=0.45 while for anomalous (Non-Fickian) transport, n ranges between 0.45 and 0.89 and for zero order release, n = 0.89. The Korsmeyer-Peppas model was plotted between log cumulative % drug releases versus log time.

3.0 RESULT AND DISCUSSION

3.1 Preformulation studies

These investigations are a necessary part of the development process for a stable, reliable dosage form. By using a variety of analytical techniques, including melting point, solubility, melting spectroscopy, and UV/IR spectroscopy, the acquired drug sample was identified.

3.1.1 Organoleptic properties

Organoleptic properties of drug Ciclopirox Olamine found to be as per B.P. monograph. The Organoleptic properties of Ciclopirox Olamine were found to the given in table 3.1.

Table 3.1: Organoleptic properties of Ciclopirox Olamine

Properties	Description
Form	Crystalline Powder
Odor	Odorless
Color	White or almost white

3.1.2 Melting point

Table 3.2: Data of Ciclopirox Olamine Melting Point

Drug	Specification	Observation
Ciclopirox Olamine	140-150°C	142.33°C±0.577

Discussion: The melting point of Ciclopirox Olamine was found to be 142.33°C±0.577; hence drug sample was free from any type of impurities.

3.1.3 UV Spectroscopy

3.1.3.1. Determination of absorption maxima

The result of UV spectrum of Ciclopirox Olamine is shown in Figure 3.1.

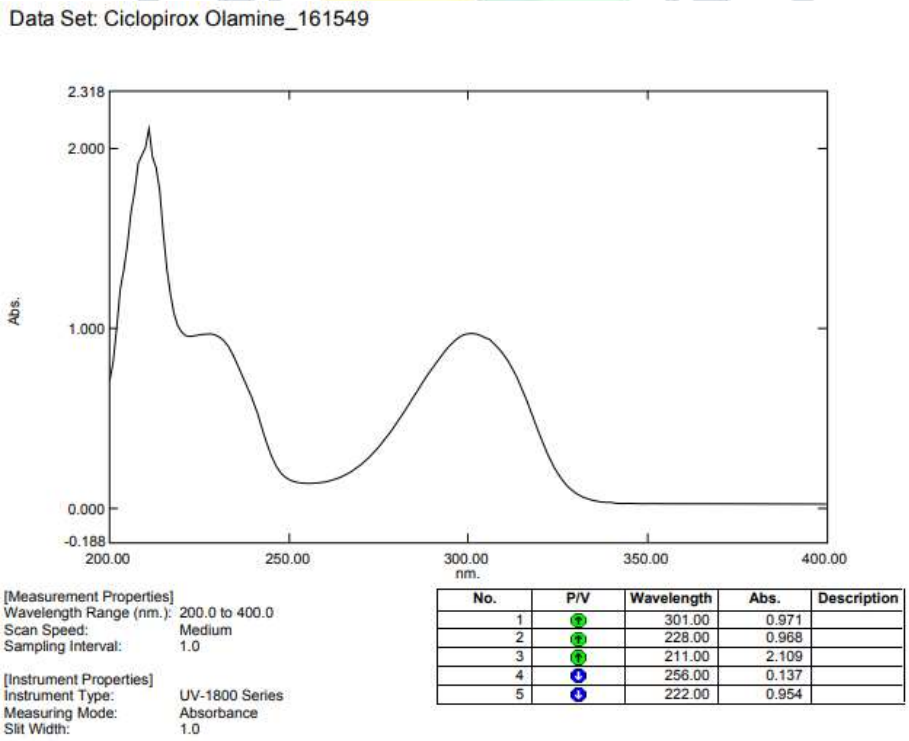

Figure 3.1: UV spectrum of Ciclopirox Olamine in methanol

Discussion: The maximum wavelength of Ciclopirox Olamine was observed at 301nm in methanol which is found to be similar with reference standards.

3.1.3.2 Preparation of calibration curve of Ciclopirox Olamine in methanol

Table 3.3: Calibration curve of Ciclopirox Olamine

Sr.no.	Concentration µg/ml	Absorbance
1	5	0.163±0.001
2	10	0.272±0.002
3	15	0.404±0.002
4	20	0.543±0.002
5	25	0.678±0.001
6	30	0.825±0.001
7	35	0.968±0.002

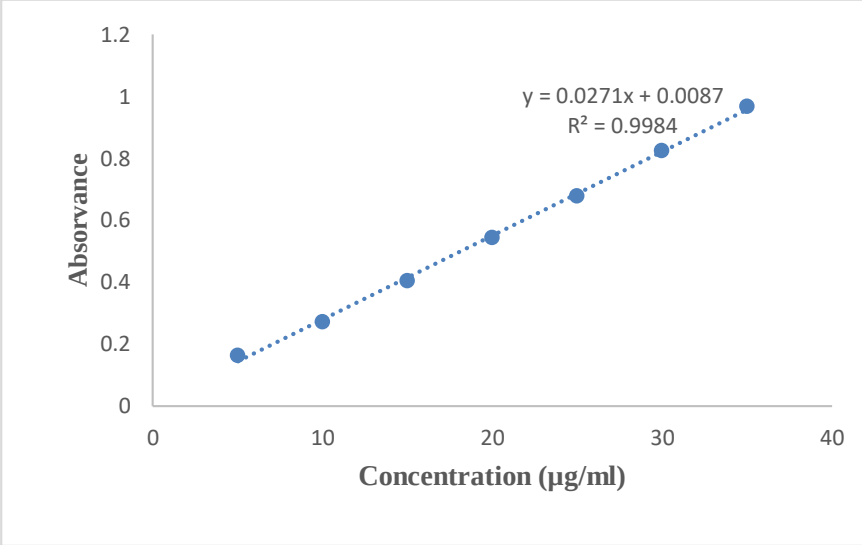

Figure 3.2: Calibration curve of Ciclopirox Olamine in methanol

Discussion: The calibration curve for Ciclopirox Olamine was obtained by using the 5 to 35µg/ml concentration of Ciclopirox Olamine in methanol. The absorbance was measured at 301nm. The standard curve of Ciclopirox Olamine as shown in graph indicated the regression equation y=0.0271x + 0.0087 and R^2 value is 0.998, which shows good linearity as shown in table 3.3, respectively.

3.1.4 Partition coefficient determination

The shake flask method was used to carry out the research on partition coefficient determination.

Table 3.4: Partition coefficient of Ciclopirox Olamine

Drug	Solvent system	Partition coefficient (log P)
Ciclopirox Olamine	n-octanol:water	2.25± 0.014

(Mean ± SD, n=3)

Discussion: The partition coefficient of Ciclopirox Olamine in n- Octanol: Water was found to be; 2.25± 0.014 which was found similar to the literature. This indicates that the drug Ciclopirox Olamine is lipophilic in nature.

3.1.5 Solubility studies

Solubility of drug in various solvents were carried out in order to screen for the components to be used for formulation development as shown in table 3.5

Table 3.5: Solubility profile of Ciclopirox Olamine in different solvent

Sr. no.	Solvent	Solubility (mg/ml)	Solubility
1	Methanol	34.16±0.77	Soluble
2	Water	11.278±0.14	Sparingly Soluble
3	Phosphate buffer saline pH 7.4	32.077±0.03	Soluble
4	Ethanol	35.066±0.184	Soluble

(Mean ± SD, N=3)

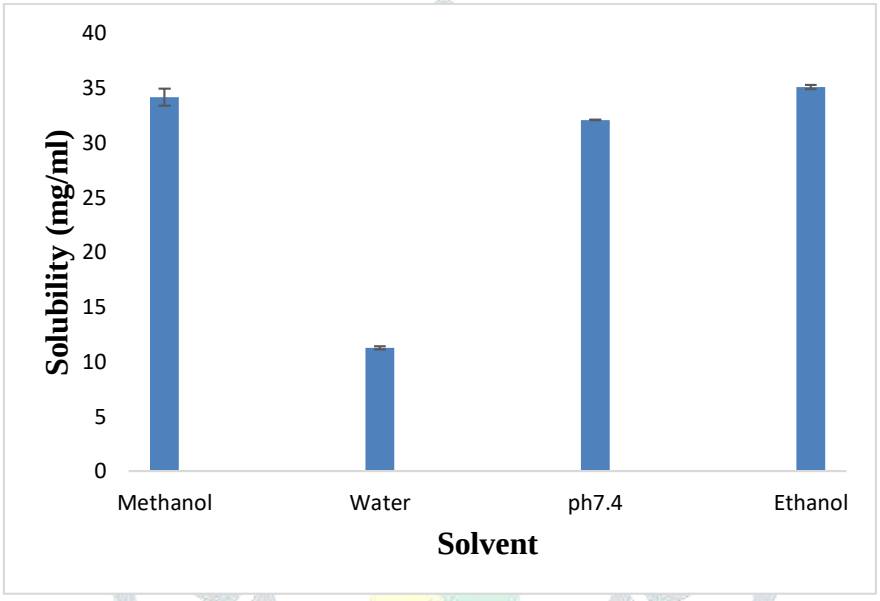

Figure 3.3: Solubility profile of Ciclopirox Olamine in different solvent

Discussion: From the above data, it is clearly seen that Ciclopirox Olamineis highly soluble in ethanol and followed by methanol (figure 3.3 and table 3.5).

6.1.6 FTIR analysis of pure drug and excipient

The FTIR spectrum and its interpretation Ciclopirox Olamineis shown in figure 3.4-3.8 and table 3.6-3.9, respectively.

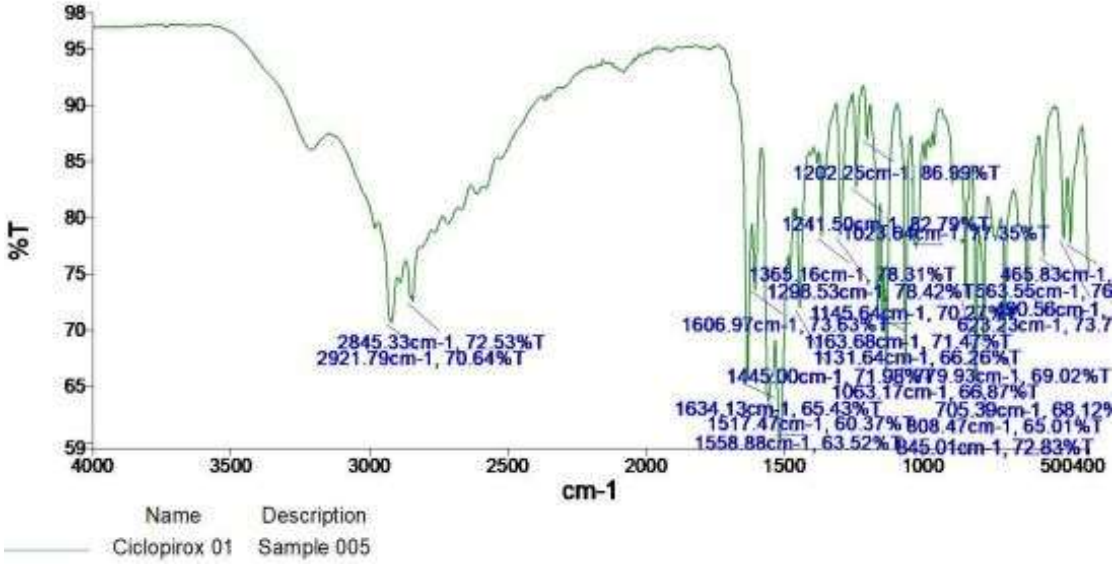

Figure 3.4: FTIR spectrum of Ciclopirox Olamine

Table 3.6: Interpretation of FTIR spectrum of Ciclopirox Olamine

Reported peak (cm-1)	Observed peak (cm-1)	Functional group
2922.26	2921.79	C-H stretching
2852.72	2845.33	C-H stretching
1535.34	1558.88	C=C stretching
1634.13	1637.56	C=O stretching
1444.68	1445.00	C-C stretching

The FTIR spectra of Ciclopirox Olamine were shown in the **Figure 3.4**; **Table 3.6**.The principal IR absorption peaks of Ciclopirox olamine at 2921.79 and 2845.33cm^{-1}(C–H stretching),1558.88 cm^{-1}(C=C stretching), and 1637.56cm^{-1}(C=O stretching),1445.00cm^{-1}(C-C stretching) were all observed in the spectra of Ciclopirox olamine. These observed principal peaks. This observation confirmed the purity and authenticity of the Ciclopirox Olamine. The principal IR absorption peaks of Ciclopirox olamine.

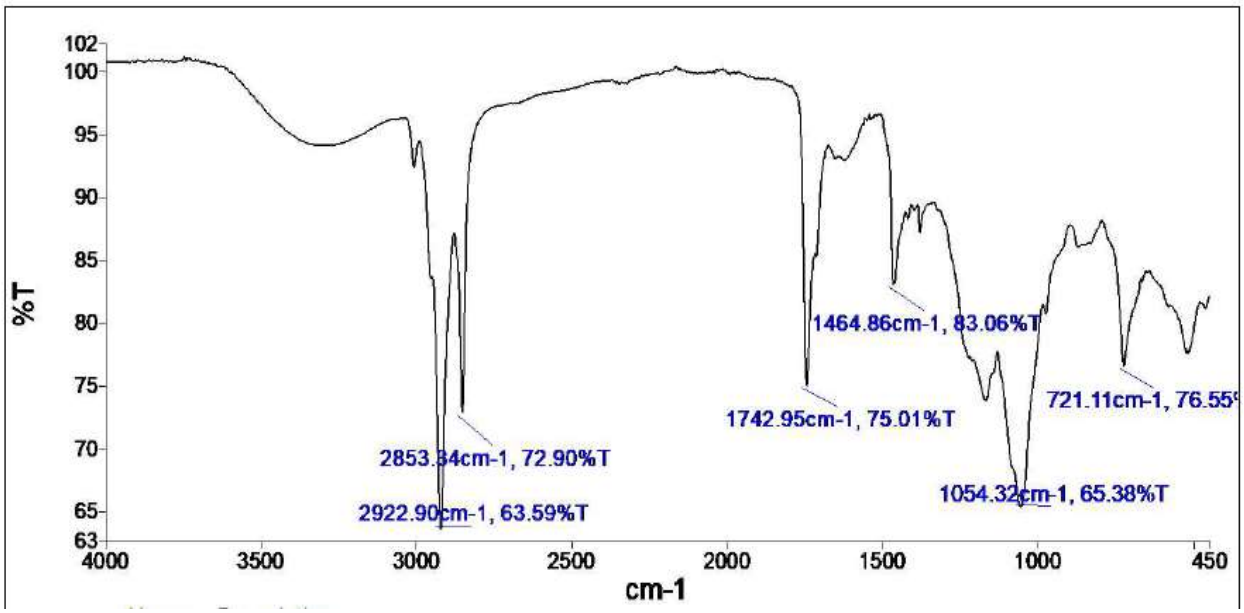

Figure 3.5: FTIR spectrum of Phospholipid

Table 3.7: FTIR interpretation of Phospholipid

Reported peak (cm-1)	Observed peak (cm-1)	Functional group
2918.3 and 2854.96	2922.90 and 2853.34	C–H stretching band of long fatty acid chain
1728.22	1742.95	Carbonyl stretching band in the fatty acid ester
1093.65	1054.32	P–O–C stretching band

The FTIR spectra of Phospholipid were shown in the **Figure 3.5**; **Table 3.7**. The principal IR absorption peaks of Phospholipid at 2922.90 and 2853.34cm^{-1} (C–H stretching band of long fatty acid chain), 1742.95cm^{-1} (Carbonyl stretching band in the fatty acid ester), and 1054.32cm^{-1} (P–O–C stretching band) were all observed in the spectra of Phospholipid. These observed principal peaks. This observation confirmed the purity and authenticity of the Phospholipid.

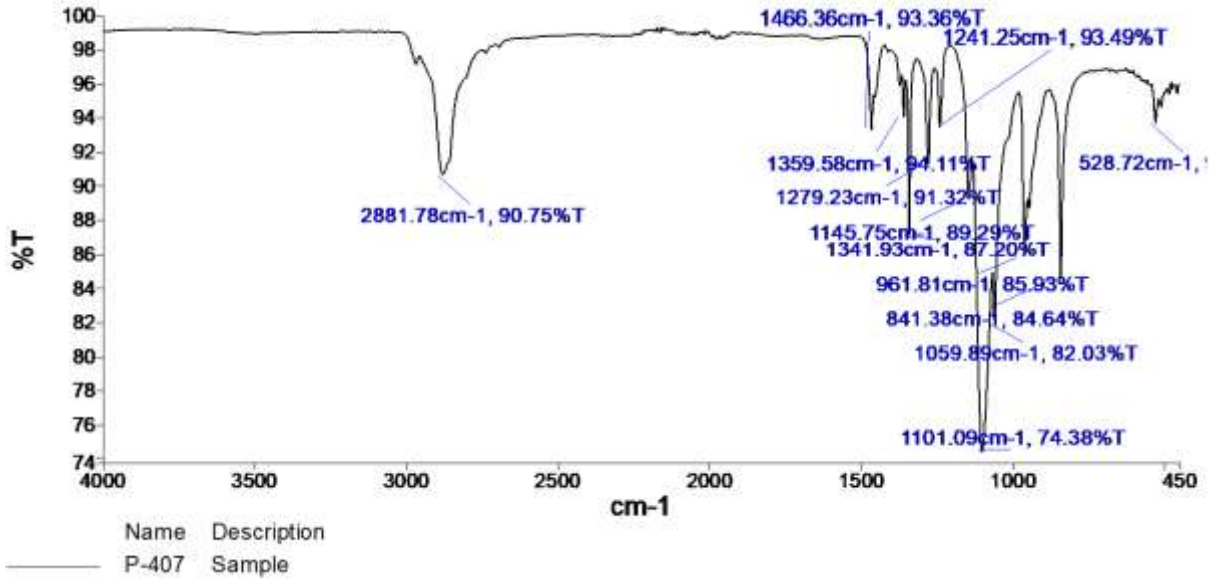

Figure 3.6: FTIR spectrum of Poloxamer 407

Table 3.8: Interpretation of FTIR spectrum of Poloxamer 407

Reported peak (cm^{-1})	Observed peak (cm^{-1})	Functional group
2893.02	2881.78	C-H stretch aliphatic
1355.86	1359.58	In-plane O-H bend
1124.42	1145.75	C-O stretch

Discussion: The FTIR spectra of Poloxamer 407 were shown in the figure 3.6 and table 3.8. The principal IR absorption peaks of Poloxamer 407 at 2881.78cm–1 (C-H stretch aliphatic), 1359.58cm–1 (in-plane O-H bend), oand 1145.75cm–1 (C-O stretch) were all observed in the spectra of Poloxamer 407 were found to be similar to cited peaks. These observed principal peaks confirmed the purity and authenticity of the Poloxamer 407.

3.1.7 Drug excipient compatibility study by FTIR spectroscopy

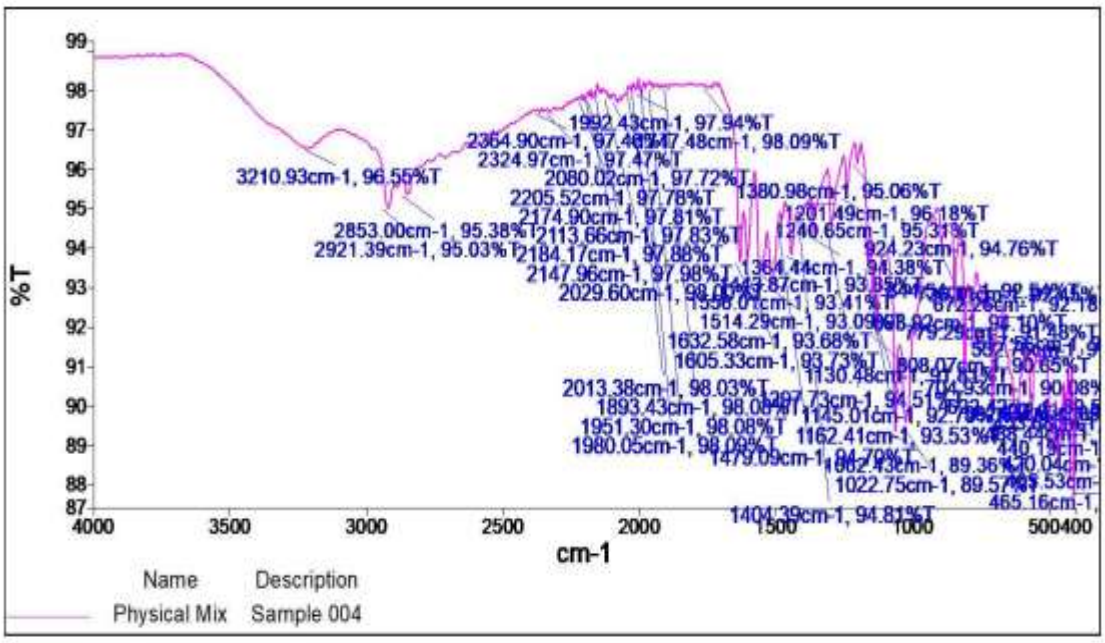

Figure 3.7: FTIR spectrum of Physical mixture

Table 3.9: Interpretation of FTIR spectrum of Physical mixture

Reported peak (cm-1)	Observed peak (cm-1)	Functional group
2921.79	2921.39	C-H stretching
2845.33	2853.00	C-H stretching
1558.88	1556.01	C=C stretching
1637.56	1632.58	C=O stretching
1445.00	1443.87	C-C stretching

Discussion: FTIR of physical mixture (**Figure 3.7 and Table 3.9**) were carried out to eliminate the possibility of interaction between drug and excipients used with analytical method of drug estimation. All the spectrum peaks revealed that corresponding peaks of drugs are present in the above spectra along with excipients peaks. Hence no interaction was observed in this mixture.

3.2. Preparation of Ciclopirox Olamine Micellar nanocarrier formulation

3.2.1. Visual Appearance

The visual appearance of Ciclopirox Olamine Micellar nanocarrier formulation is shown in table 3.10.

Table 3.10: Visual appearance of different Ciclopirox Olamine Micellar nanocarrier formulation

Formulation code	Visual Appearance
F1	Homogeneous dispersion form
F2	Homogeneous dispersion form
F3	Homogeneous dispersion form
F4	Homogeneous dispersion form
F5	Homogeneous dispersion form
F6	Homogeneous dispersion form
F7	Homogeneous dispersion form

Discussion: The results indicate that formulating the Micellar nanocarrier formulation show good appearance and no phase separation were produced in all batches. On the basis all formulation was selected for further evaluation.

3.2.2. Percentage Drug Entrapment

Percentage Drug Entrapment of all formulation was given in a table 3.11.

Table 3.11: Percentage Drug Entrapment of Ciclopirox Olamine Micellar nanocarrier formulation

Sr. No.	Formulation Code	% Entrapment Efficiency
1	F1	72.043±0.073
2	F2	78.292±0.074
3	F3	75.770±0.113
4	F4	80.936±0.149
5	F5	85.672±0.194
6	F6	89.829±0.113
7	F7	79.927±0.525

Value is expressed as mean ± SD; n = 3

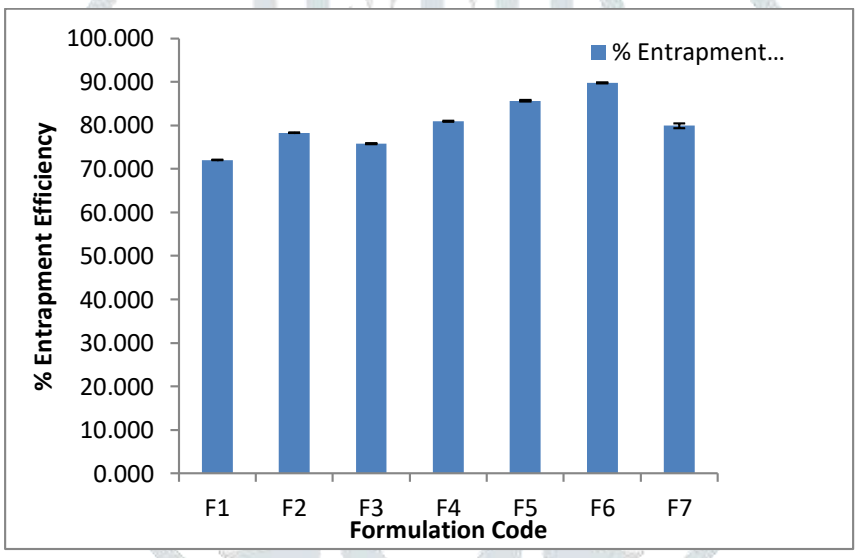

Figure 3.8: Percentage Drug Entrapment of Ciclopirox Olamine Micellar nanocarrier formulation

Discussion: From the table 3.11, it was found that Percentage Drug Entrapment of all formulation was found to be in a range 72.043±0.073 to 89.829±0.113. These results explain that there is a significant effect on percent drug content was observed with polymer concentration. Maximum percentage drug entrapment was found of formulation F6 that was 86.791±0.146.

3.2.3. Particle size distribution & Zeta potential

Particle Size

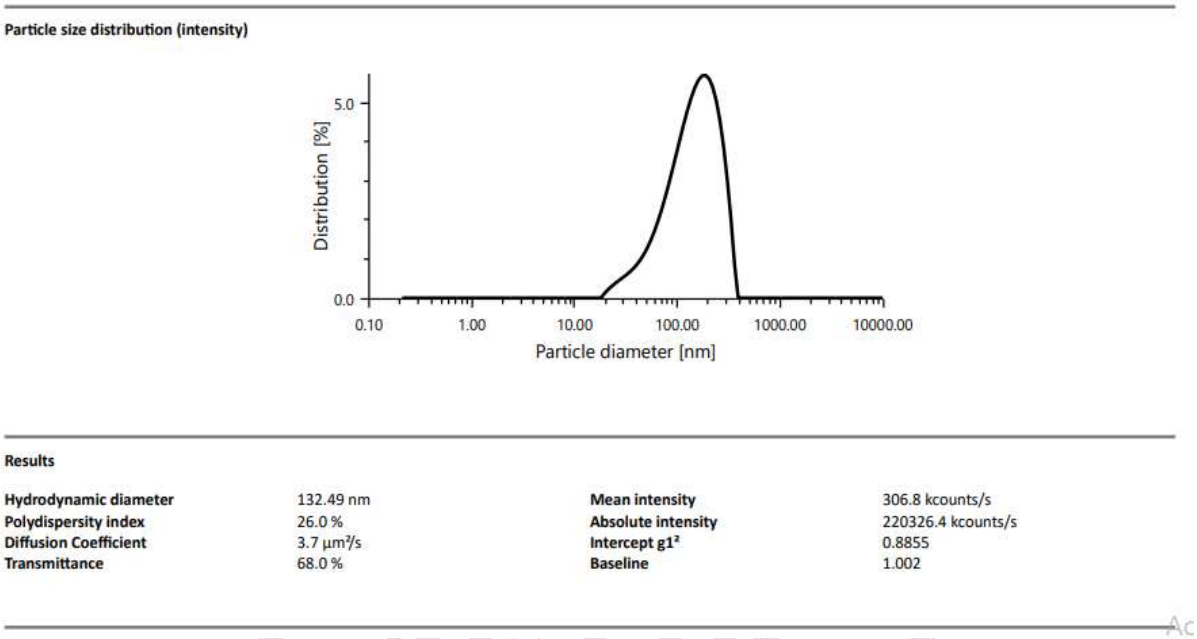

Figure 3.9: Particle size peak of F6 formulation

Discussion: Figure 3.9 demonstrated particle size of F6 formulation was 132.49nm with PDI 0.260.

3.2.3.1 Zeta Potential

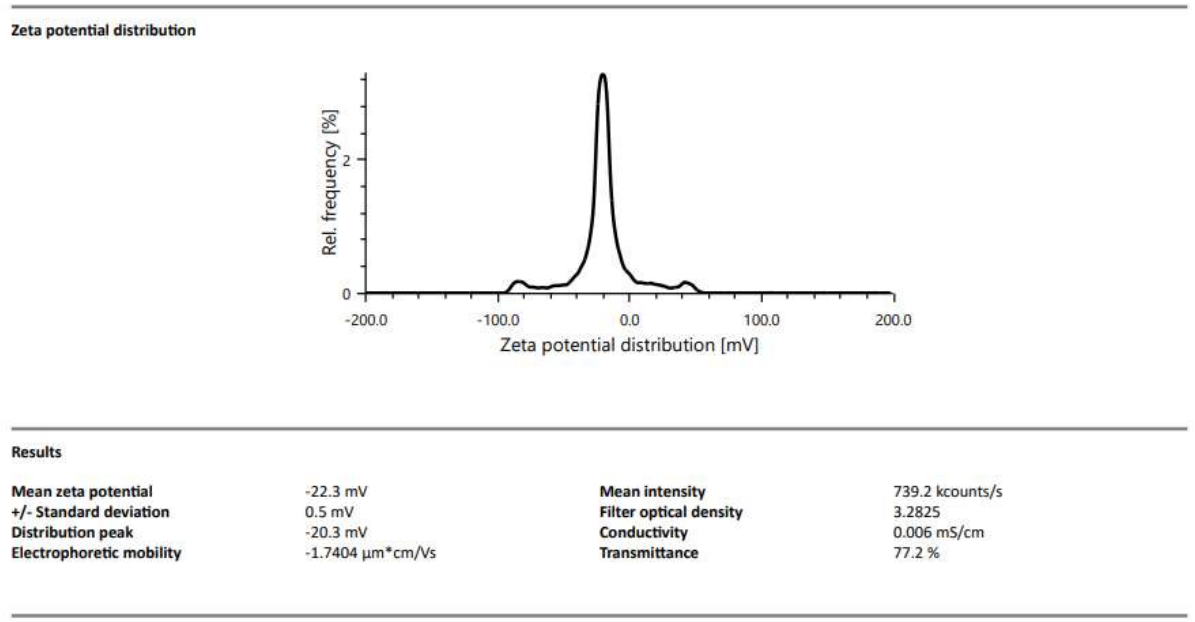

Figure 3.10: Zeta potential graph of F6 formulation

Discussion: Figure 3.10 demonstrated zeta potential of F6 formulation was -22.3mV represents stability of formulation.

3.2.4 TEM of Ciclopirox Olamine Micellar nanocarrier formulation (F6)

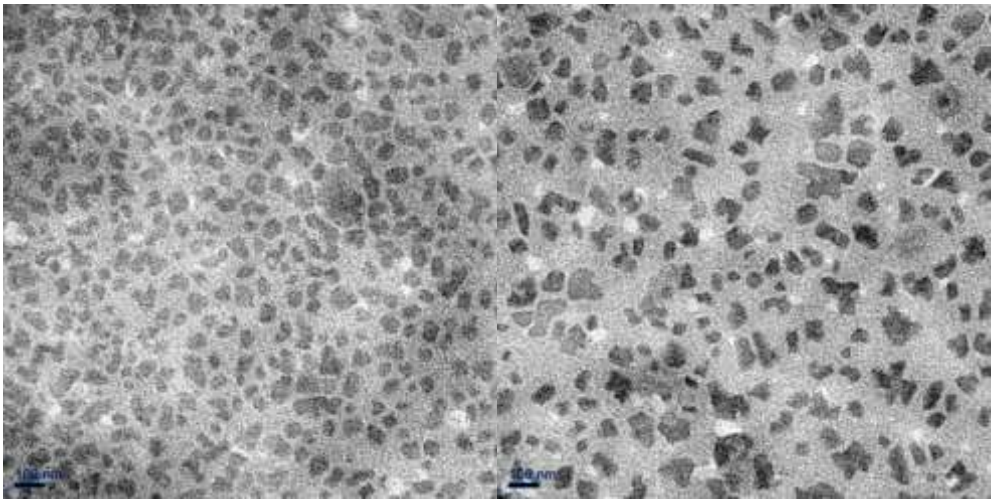

Figure 3.11: TEM Image of Formulation F6

Discussion: The TEM pictures were shown in figure 3.11. The prepared Ciclopirox Olamine Micellar formulation of the optimized formulation (F6) was found to be irregular cuboidal morphology of the micelles. The length and diameter of the micelles are in the nano range.

On the basis of particle size, visual appearance, TEM & % entrapment efficiency, F6 formulation was selected as further study.

3.3. Evaluation of Ciclopirox olamine-loaded polymeric micelles shampoos

3.3.1 Organoleptic Properties

Table 3.12: Visual Appearance of Ciclopirox olamine-loaded polymeric micelles shampoos

Sr. no.	Formulation code	Color	Clarity	Odor	Texture
1	F8	Pale Yellow	Cloudy	Pleasant	Gel Type
2	F9	Pale Yellow	Cloudy	Pleasant	Gel Type

Discussion: The results of organoleptic evaluations are shown in table 3.12. In the formulated shampoos, we did not add any color or fragrance. However, the presence of lanolin resulted in pale yellow colored shampoo formulations.

3.3.2 Determination of pH

Table 3.13: pH study of Shampoos

Sr. no.	Formulation code	pH (Mean ± S.D)
1	F8	5.78±0.02
2	F9	5.67±0.19

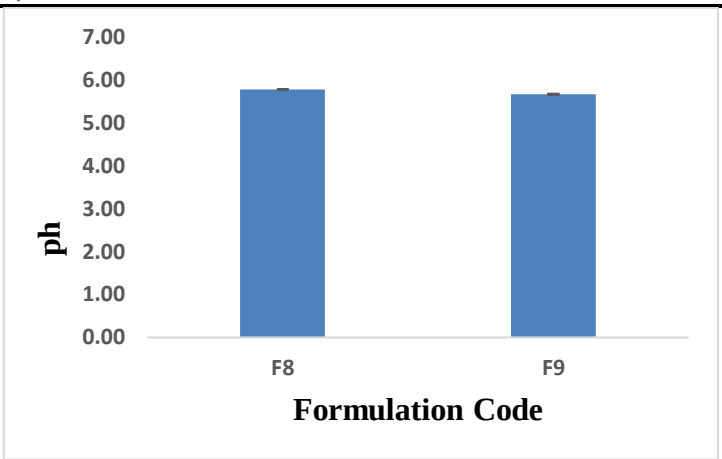

Figure 3.12: pH of Shampoos

Discussion: From the Table 3.13 & fig. 3.12, it was found that pH of all formulation was found to be in a range 5.67±0.19 to 5.78±0.02.

3.3.3 Viscosity

Table 3.14: Viscosity Study of formulations (F8-F9)

Sr. no.	Formulation code	Viscosity (cps) (Mean ± S.D)
1	F8	2254.33±6.06
2	F9	2690.00±5.86

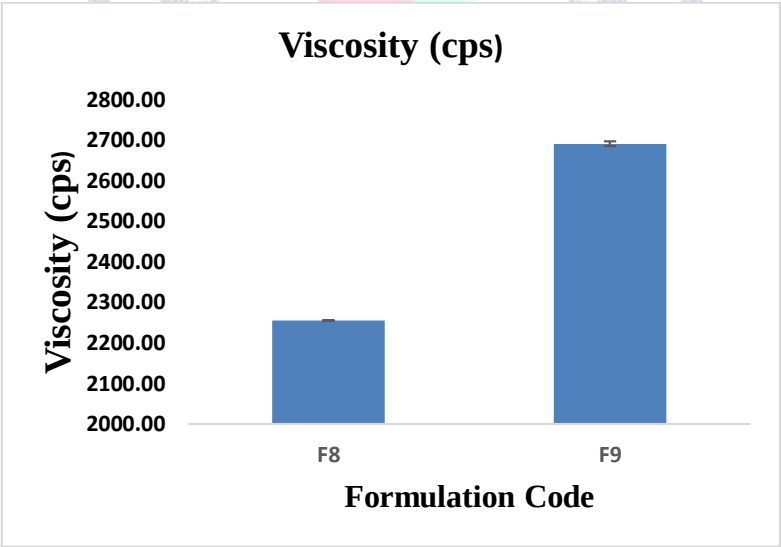

Figure 3.13: Viscosity Study of formulations (F8-F9)

Discussion: The viscosity of all the formulation was in range of 2254.33±6.06 and 2690.00±5.86. (**Table 3.14 and Figure 3.13)**

3.3.4 Solid content determination

Table 3.15: Solid content Study of formulations (F8-F9)

Sr. no.	Formulation code	% Solid content (mean ± SD)
1	F8	25.314±0.23
2	F9	27.426±0.46

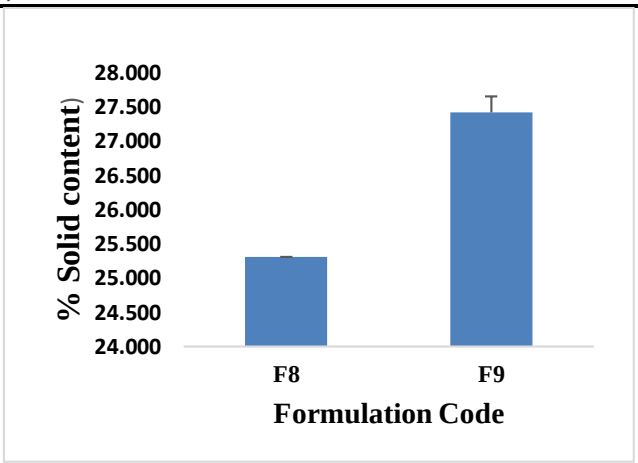

Figure 3.14: Solid content Study of formulations (F8-F9)

Discussion: The Solid content of all the formulation was in range of 25.314±0.23 and 27.426±0.46. (**Table 3.15 and Figure 3.14)**.

3.3.5 Foam Volume

Table 3.16: Foam Volume of formulations (F8-F9)

Time (Min.)	Formulation Code	
	F8	**F9**
1	172	180
2	170	178
3	169	175
4	166	172
5	164	171

Discussion: Foaming ability and foam stability although foam generation has little to do with the cleansing ability of shampoos, it is of paramount importance to the consumer and is therefore an important. All the shampoos showed similar foaming characteristics in distilled water. The foam stability of shampoos is listed in table 3.16. The final formulation produced stable foams there was little bet change in foam volume.

3.3.6 Dirt Dispersion

Table 3.17: A comparison of dirt dispersion of formulations (F8-F9)

Formulation Code	Dirt Dispersion
F8	Clear
F9	Clear

Discussion: Shampoo that cause the ink to concentrate in the foam is considered poor quality, the dirt should stay in water. Dirt that stays in the foam will be difficult to rinse away. It will redeposit on the hair. All shampoos showed similar results. These results indicate that no dirt would stay in the foam; so prepared formulations are satisfactory.

3.3.7 Wetting Dispersion

Table 3.18: A comparison of wetting time of formulations (F8-F9)

Sr. no.	Formulation code	Wetting Time (Seconds) (mean ± SD)
1	F8	4.650±0.12
2	F9	5.567±0.21

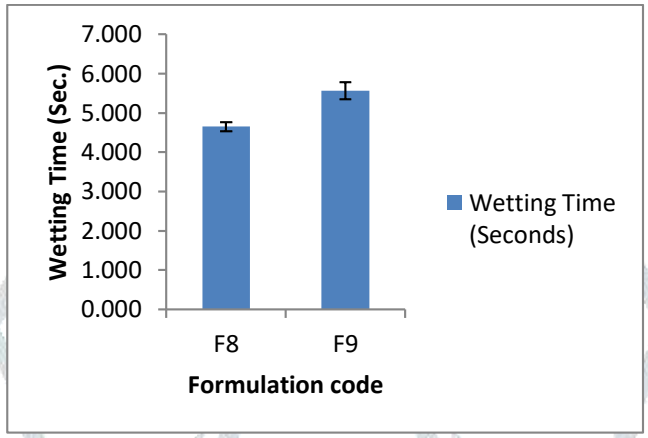

Figure 3.15: Wetting time Study of formulations (F8-F9)

Discussion: The wetting ability of shampoos describes their efficacy as cleansing products and it depends on the surfactant used. The formulated shampoos showed wetting time in the range of 4.650±0.12 to 5.567±0.21s (Table 3.18).

3.3.8 FTIR Spectra of final formulation

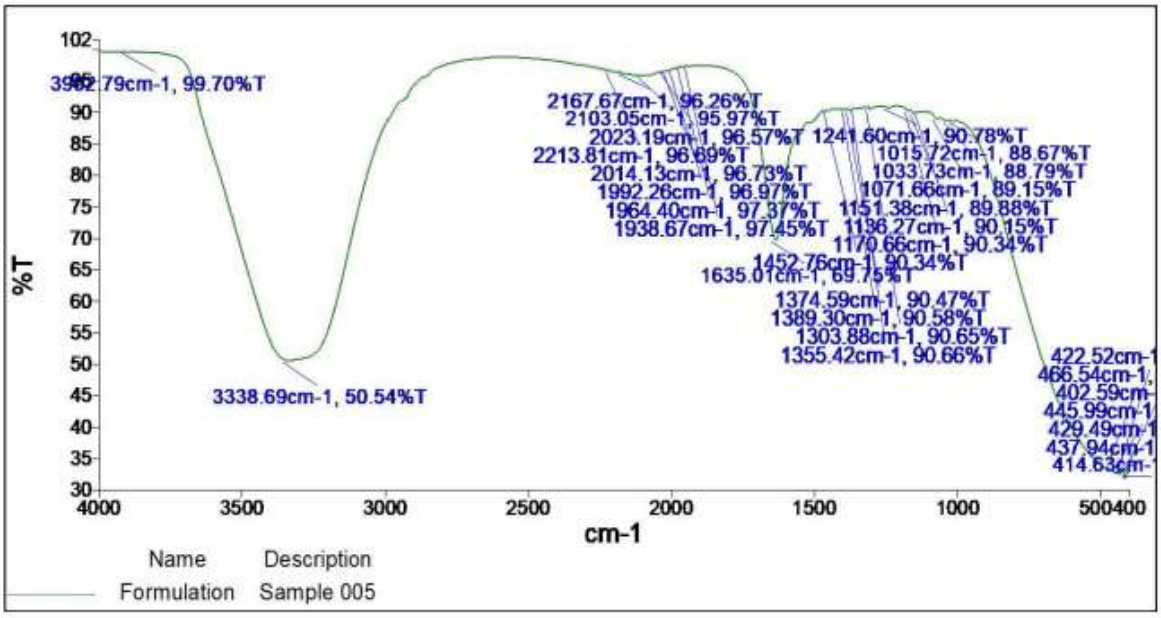

Figure No. 3.16: FTIR Spectra of Formulation F8

Discussion: The FT-IR spectra of final formulation indicate that characteristic peak of Ciclopirox was not visible in the formulation spectra which indicates that drug was completely encapsulate in the micelles.

3.3.9 In vitro drug release studies

Table 3.19: In vitro drug release of Ciclopirox olamine-loaded polymeric micelles shampoos formulations

Sr. No.	Time (Hrs)	Drug Release of Formulation F8 (%)	Drug Release of Formulation F9 (%)
1	0	0	0
2	0.25	4.306±0.507	4.860±0.691
3	0.5	12.720±0.332	10.063±0.332
4	1	22.461±0.691	18.033±0.664
5	2	38.181±0.507	32.978±0.332
6	4	55.450±0.192	48.144±0.507
7	6	67.959±0.691	61.317±0.691
8	8	78.476±0.332	71.945±0.192
9	10	88.771±0.879	79.362±0.507
10	12	93.642±0.192	84.011±0.691

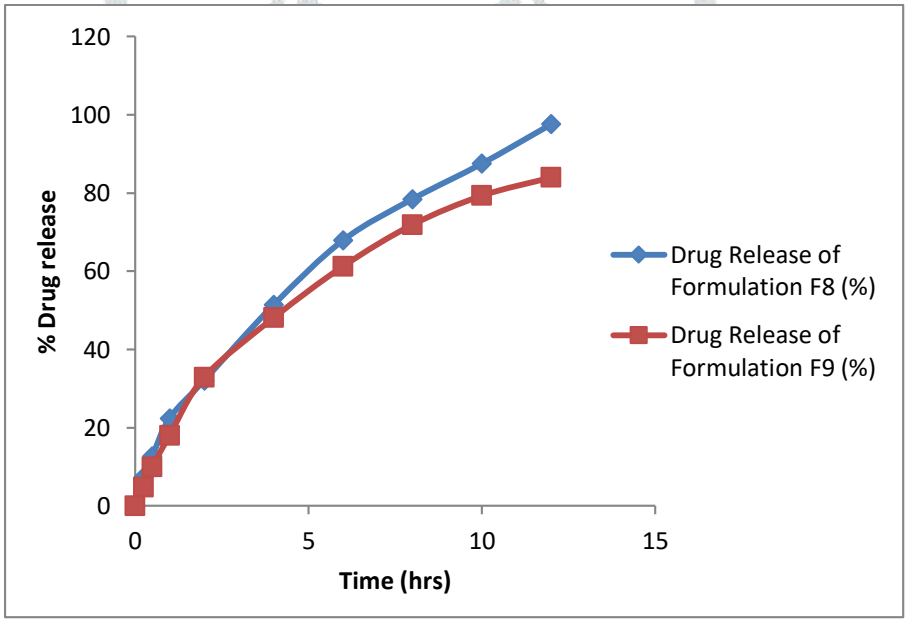

Figure 3.17: Percentage drug release of Ciclopirox olamine-loaded polymeric micelles shampoos formulations

Result: The in-vitro drug release of a Ciclopirox olamine-loaded polymeric micelles shampoos formulations F8 & F9 was given in a Table 3.19 and figure 3.17. In case of F8 formulation release was 93.642±0.192% within 12hrs. On the other hand, the release of formulations (F9) was 84.011±0.691within 12hrs. Hence it can be observed that the release rate of formulation F8 is maximum and gives a control drug release.

3.3.10 Drug release kinetic studies

3.3.10.1 Zero order kinetics

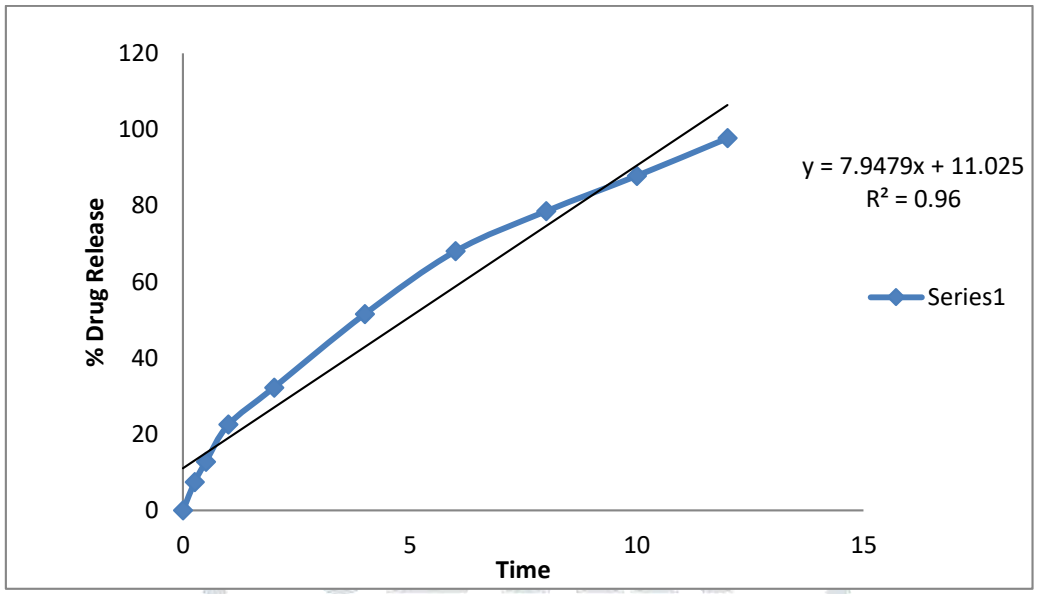

Figure 3.18: Zero order graph of formulation F8

3.3.10.2 First order kinetics

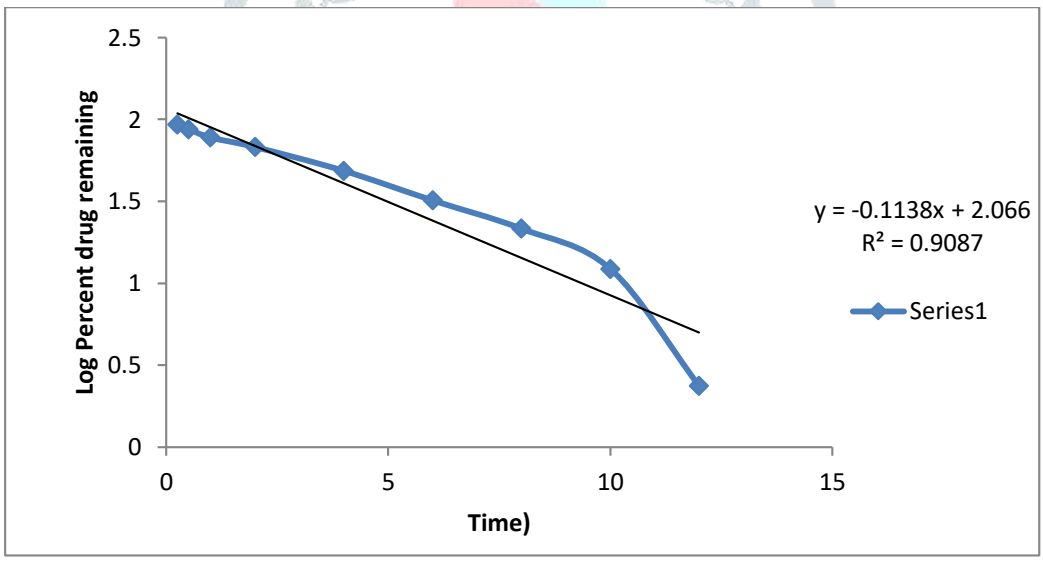

Figure 3.19: First order graph of formulation F8

3.3.10.3 Higuchi's Model

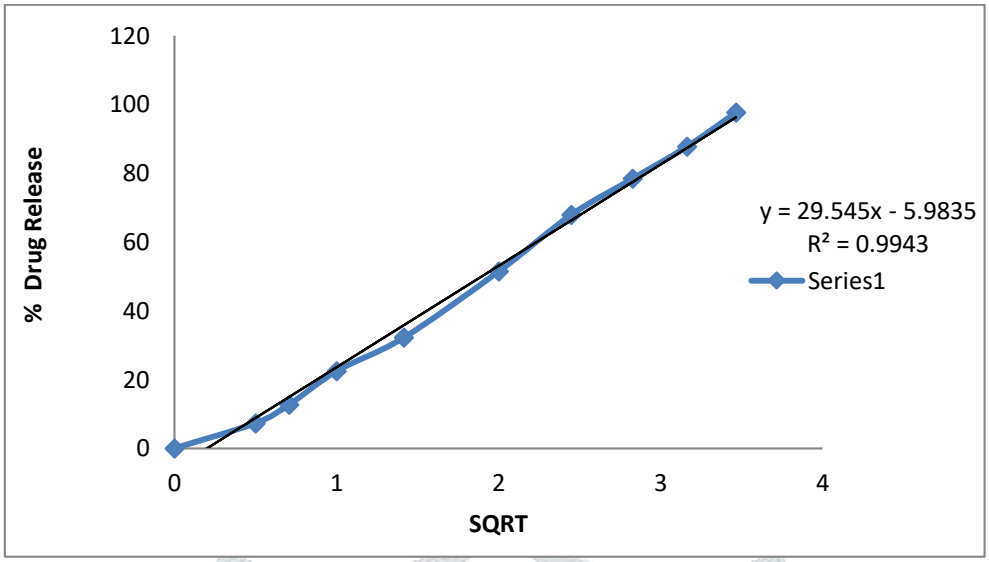

Figure 3.20: Higuchi order graph of formulation F8

3.3.10.4 Korsmeyer-Peppas Model

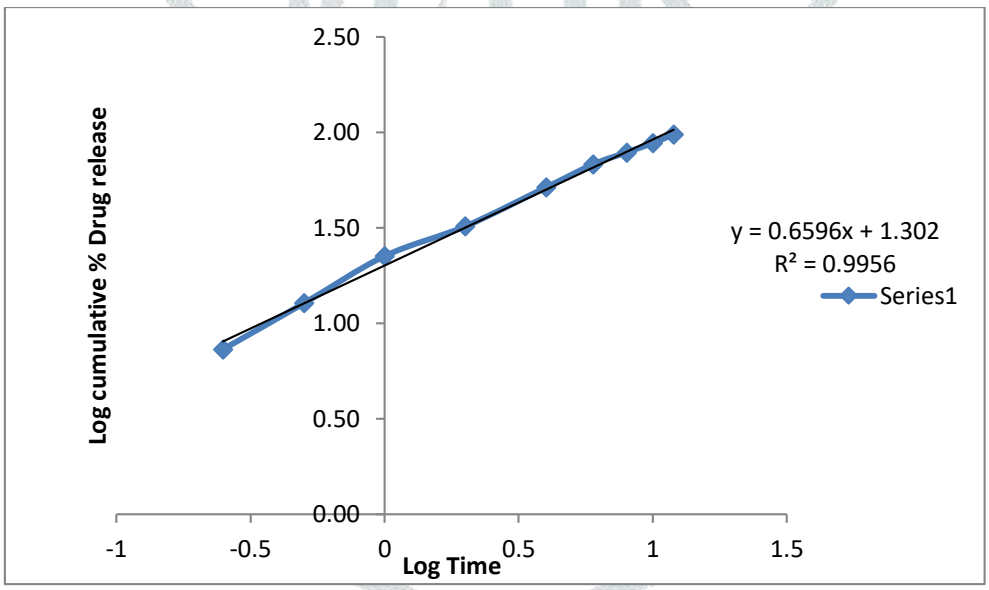

Figure 3.21: Korsmeyerpeppas order graph of formulation F8

Table 3.20: Kinetic equation parameter of formulation F8

Formulation Code	Zero order		First order		Higuchi		K. Peppas	
	K_0	R^2	K_0	R^2	K_0	R^2	K_0	R^2
F8	7.9479	0.96	-0.1138	0.9087	29.545	0.9943	0.6596	0.9956

Mathematical models are commonly used to predict the release mechanism and compare release profile. For the optimized formulation, the % drug release vs time (zero order), log percent drug remaining vs time (first order), log per cent drug release vs square root of time (Higuchi plot), and log of log % drug release vs. log time (Korsmeyer and Peppas Exponential Equation) were plotted. In each case, R^2 value was calculated from the graph and reported in **Table 3.20** and **Figure 3.18 to Figure 3.21.** Considering the determination coefficients, K. Peppas model was found (R^2=0.9956) to fit the release data best. It could be concluded from the results that the drug was released from polymeric micelles shampoo formulation F8 by a controlled mechanism.

4.0 Summary and Conclusion

Shampoo is a hair care product that is use for cleansing of hair and nourishing them and making them protective against outer environment. It removes oil, dirt, dandruff and other particles. So basically Ciclopirox shampoo helps for the treatment of fungus in the scalp which is also called as seborrhoeic dermatitis. Vesicles are closed bilayer self-assemblies of amphiphiles which have capabilities to hold the variety of drug molecules within their interiors. The results of the present investigation showed that the problems associated with the ciclopirox conventional formulation could be overcome by incorporating it into a new transdermal ultraflexible drug carrier, micelles.

Before micelles development, preformulation studies were carried out to characterize the chemical and physical properties of drug substance. The FT-IR spectrum of drug samples was found to be in concordant with the reference chemical groups present in the structure of the ciclopirox olamine. The UV spectrum of ciclopirox olamine in Methanol exhibited a broad band at 301nm. The correlation coefficients were found to be 0.998 for ciclopirox which is closed to one indicated for good linearity. The melting point was determined by capillary method which complies with the melting point given in reference. The solubility results showed that ciclopirox highly soluble in ethanol and followed by methanol. The solubility profile of drug in different solvents shows that drug is lipophilic in nature which is further confirmed by the partition coefficient study. The preformulation study (FT-IR spectrum, UV spectrum and melting point) results suggested that ciclopirox was pure and good in quality and the estimation procedure was found to be quite reliable, accurate and suitable for formulation development.

Micellar nanocarrier formulation of ciclopirox was prepared by a thin film hydration method. For optimization, different formulations (F1 to F7) were prepared using different concentration of Phosphatidylcholine and Pluronic. The percentage Drug Entrapment of all formulation was found to be in a range 72.043±0.073 to 89.829±0.113. Formulation (F6) with maximum entrapment efficiency, good appearance & size considered as optimized formulation. The shape of the optimized F6 formulation was confirmed through TEM and particle size & Zeta potential measured by particle size analyzer and found that most of the particles were well identified.

The optimal formulation (F6) was selected to preparation of shampoos. The prepared shampoos formulations F8 & F9 were examined visually for their consistency and found to pale yellow colored shampoo gel type appearance. The pH of all formulation was found to be in a range 5.67±0.19 to 5.78±0.02. Viscosity of all the formulation was in range of 2254.33±6.06 and 2690.00±5.86 & Solid content of all the formulation was in range of 25.314±0.23 and 27.426±0.46. All the shampoos showed similar foaming characteristics in distilled water. The final formulation produced stable foams there was little bet change in foam volume and the dirt dispersion study results indicate that no dirt would stay in the foam; so prepared formulations are satisfactory. The formulated shampoos showed wetting time in the range of 4.650±0.12 to 5.567±0.21s. The FT-IR spectra of final formulation indicate that characteristic peak of Ciclopirox was not visible in the formulation spectra which indicates that drug was completely encapsulate in the micelles. The in-vitro drug release of a Ciclopirox olamine-loaded polymeric micelles shampoos formulations F8 & F9 shows 93.642±0.192% & 84.011±0.691% within 12hrs. Hence it can be observed that the release rate of formulation F8 is maximum and gives a control drug release. To know precisely, the rate and mechanism of drug release, the *in vitro* data was fitted to zero order, first order, Higuchi and Korsmeyer-Peppas model. The results showed that the drug release of F8 formulation followed Korsmeyer and Peppas order which describes that the Ciclopirox olamine-loaded polymeric micelles shampoo formulation F8 by a controlled mechanism.

Thus, it can be concluded from the result obtained that the micelles shampoo formulation formulation developed for scalp delivery of ciclopirox possessed better skin permeation potential, and higher entrapment efficiency, as well as had ability as a self-penetration enhancer.

Reference

1. Al Badi, K.; Khan, S.A. Formulation, evaluation and comparison of the herbal shampoo with the commercial shampoos. Beni-Suef University Journal of Basic and Applied Sciences, 2014, 3(4), 301- 305
2. A, Wagner N, Chatelus A, Shroot B, Schaefer H. Site-specific drug delivery to pilosebaceous structures using polymeric microspheres. *Pharm Res*. 1993;10:1738–1744.

3. Aghel, N.; Moghimipour, E.; Raies Dana, A. Formulation of a herbal shampoo using total saponins of Acanthophyllum squarrosum. Iran. J. Pharm. Res., 2010, (3), 167-172.
4. Ajay Mandal. "Experimental investigation of PEG 6000/Tween 40/SiO2 NPs stabilized nanoemulsion properties: a versatile oil recovery approach." Journal of Molecular Liquids 319 (2020): 114087.
5. Ali J, Khar R, Ahuja AA textbook of dosage form design. Birla publications Pvt Ltd, Delhi; 3rd edition,.(2008);100-107.
6. Anestopoulos, I.; Kiousi, D.; Klavaris, E.A.; Galanis, A.; Salek, K.; Euston, S.R.; Pappa, A.; Panayiotidis, M.I. Surface active agents and their health-promoting properties: Molecules of multifunctional significance. *Pharmaceutics* 2020, *12*, 688. [Google Scholar]
7. Ansari, M.J. An overview of techniques for multifold enhancement in solubility of poorly soluble drugs. *Curr. Issues Pharm. Med. Sci.* 2019, *32*, 203–209. [Google Scholar]
8. Anselmo, A.C.; Mitragotri, S. Nanoparticles in the clinic: An update. *Bioeng. Transl. Med.* 2019, *4*, e10143. [Google Scholar]
9. Aslam, J.; Lone, I.H.; Radwan, N.R.E.; Siddiqui, M.F.; Parveen, S.; Alnoman, R.B.; Aslam, R. Molecular interaction of amino acid-based gemini surfactant with human serum albumin: Tensiometric, spectroscopic, and molecular docking study. *ACS Omega* 2019, *4*, 22152–22160. [Google Scholar]
10. Azagury A, Khoury L, Enden G, Kost J. Ultrasound mediated transdermal drug delivery. Adv Drug Deliv Rev. 2014;72:127-43.
11. Babar, A.; Kawilarang, C.; Cutie, A. J.; Plakogiannis, F. M. (1985). In-Vitro Release of Zinc Pyrithione from A Shampoo Base and the Effects of Various Additives on its Release Rate. Drug Development and Industrial Pharmacy, 11(8), 1507–1522.
12. Balaraman Harish Babu, "Task-specific deep eutectic solvent based extraction coupled cascade chromatography quantification of α-glucosidase inhibitory peptide from Ocimum tenuriflorum seeds." Microchemical Journal 157 (2020): 104883.
13. Basalious, E. B., & Shamma, R. N. (2015). Novel self-assembled nano-tubular mixed micelles of Pluronics P123, Pluronic F127 and phosphatidylcholine for oral delivery of nimodipine: In vitro characterization, ex vivo transport and in vivo pharmacokinetic studies. International Journal of Pharmaceutics, 493(1-2), 347–356.
14. Bashir, Shazia, Rawan Fitaihi, "Advances in Formulation and Manufacturing Strategies for the Delivery of Therapeutic Proteins and Peptides in Orally Disintegrating Dosage Forms." European Journal of Pharmaceutical Sciences (2023): 106374.
15. B. D. Wood. "Preparation and characterization of lipopolysaccharide (LPS) monolayers for investigating their role in bacterial adhesion." Materials Today: Proceedings 29 (2020): 895-900.
16. Bhat, I.A.; Roy, B.; Kabir-ud-Din. Micelles of cleavable gemini surfactant induce fluorescence switching in novel probe: Industrial insight. *J. Ind. Eng. Chem.* 2019, *77*, 60–64. [Google Scholar]
17. Bolzinger MA, Briançon S, Pelletier J, Chevalier Y. Penetration of drugs through skin, a complex rate-controlling membrane. Curr Opin Colloid Interface Sci. 2012;17:156–165.
18. Bourkaib, M.C.; Delaunay, S.; Framboisier, X.; Hôtel, L.; Aigle, B.; Humeau, C.; Guiavarc'h, Y.; Chevalot, I. N-acylation of L-amino acids in aqueous media: Evaluation of the catalytic performances of Streptomyces ambofaciens aminoacylases. *Enzyme Microb. Technol.* 2020, *137*, 109536. [Google Scholar]
19. Burnette, R.R. and Ongpipattanakul, B. (1988) "Characterization of the pore transport properties and tissue alteration of excised human skin during iontophoresis", J. Pharm. Sci. 77, 132–137.
20. Buttini, Francesca, et al. "Back to basics: The development of a simple, homogenous, two-component dry-powder inhaler formulation for the delivery of budesonide using miscible vinyl polymers." Journal of pharmaceutical sciences 97.3 (2020): 1257-1267.
21. C. Domb, J. L. Lebowitz, G. Gompper, and M. Schick, *Self-Assembling Amphiphilic Systems*, Phase Transitions and Critical Phenomena, Academic Press, London, UK, 1994.
22. Cevc G. Lipid vesicles and other colloids as drug carriers on the skin. *Adv Drug Deliv Rev*. 2004;56:675–711.
23. Chandra, Abhishek, et al. "Rapidly dissolving lacidipine nanoparticle strips for transbuccal administration." *Journal of Drug Delivery Science and Technology* 47 (2018): 259-267.

24. Chatval GR, K A. Instrumental methods of chemical analysis. Himalya publishing house. 2006;5th edition:102-44.
25. Chourasia R, Jain SK. Drug targeting through pilosebaceous route. Curr Drug Targets. 2009;10:950–967.
26. Clarys P, Barel A. Quantitative evaluation of skin surface lipids. *Clin Dermatol*. 1995;13:307–321.
27. Dash S, Murthy PN, Nath L, Chowdhury P. Kinetic modeling on drug release from controlled drug delivery systems. Acta Pol Pharm. 2010;67(3):217-23.
28. Daulat Haleem Khan, Sajid Bashir, Patrícia Figueiredo, Hélder A. Santos, Muhammad Imran Khan, Leena Peltonen. Process optimization of ecological probe sonication technique for production of rifampicin loaded niosomes. Journal of Drug Delivery Science and Technology 50 (2019) 27–33.
29. Dey, Sanjay, et al. Cross-linking of chitosan in drug delivery. Chitosan in Drug Delivery. Academic Press, 2022. 277-299.
30. du Plessis, J., Egbaria, K., Ramachandran, C. and Weiner, N. (1992) "Topical delivery of liposomally encapsulated gamma interferon", Antiviral Res. 18, 259–265.
31. Essa EA, Bonner MC, Barry BW. Human skin sandwich for assessing shunt route penetration during passive and iontophoretic drug and liposome delivery. J Pharm Pharmacol. 2002;54:1481–1490.
32. Fouad, S. A., Shamma, R. N., Basalious, E. B., El-Nabarawi, M. M., & Tayel, S. A. (2018). Novel instantly-dispersible nanocarrier powder system (IDNPs) for intranasal delivery of dapoxetine hydrochloride: in-vitro optimization, ex-vivo permeation studies, and in-vivo evaluation. Drug Development and Industrial Pharmacy, 44(9), 1443–1450.
33. G. Casay, O. Quattrocchi, W. Hauck, A. Hernandez-Cardoso, J. Belsky. USP melting point reference standards. Evaluation of parameters that affect the melting point. USP Pharmacopeial Forum. PF39(4) 2016.
34. G. Hair follicle differentiation and regulation. Int J Dev Biol. 2004;48:163–170.
35. Ganesh G Keshavshetti, Sidramappa B Shirsand Ciclopirox Olamine-Loaded Niosomal Gel as a Topical Drug Delivery System for Fungal Infections Pharmaceutical Resonance 2019 Vol.2 - Issue 1.
36. Gauglitz GG, Schauber J. Skin: architecture and function. In: Kamolz LP, Lumenta DB, editors. Dermal Replacements in General, Burn, and Plastic Surgery: Tissue Engineering in Clinical Practice. Heidelberg: Springer; 2013:1–11.
37. Ghasemian, E., Vatanara, A., Navidi, N., & Rouini, M. R. (2017). Brain delivery of baclofen as a hydrophilic drug by nanolipid carriers: Characteristics and pharmacokinetics evaluation. Journal of Drug Delivery Science and Technology, 37, 67–73.
38. Ghosh, S.; Ray, A.; Pramanik, N. Self-assembly of surfactants: An overview on general aspects of amphiphiles. *Biophys. Chem.* 2020, *265*, 106429. [Google Scholar]
39. Grams YY, Whitehead L, Cornwell P, Bouwstra JA. Time and depth resolved visualisation of the diffusion of a lipophilic dye into the hair follicle of fresh unfixed human scalp skin. J Control Release. 2004;98:367–378.
40. Gratieri T, Martins G, Fonseca R, Lopez V. Princípios básicose aplicação da iontoforese na penetração cutânea de fármacos. Quim Nova. 2008;31(6):1490-8.
41. Grice JE, Prow TW, Kendall MAF, Roberts MS. Electrical and physical methods of skin penetration enhancement. Transdermal Top Drug Deliv Princ Pract. 2012;43-65.
42. Guy RH, Kalia YN, Delgado-Charro MB, Merino V, Lopez A, Marro D. Iontophoresis: Electrorepulsion and electroosmosis. J Control Release. 2000;64(1-3):129-32.
43. Hadgraft, J., Walters, K.A. and Wotton, P.K. (1986) "Facilitated percutaneous absorption: a comparison and evaluation of two in vitro models", Int. J. Pharm. 32, 257–263.
44. Hordinsky M. Advances in hair diseases. *Adv Dermatol*. 2008;24:245–259.
45. https://go.drugbank.com/salts/DBSALT001147
46. https://pubchem.ncbi.nlm.nih.gov/compound/Ciclopirox-olamine
47. https://pubchem.ncbi.nlm.nih.gov/compound/poloxamer%20407

48. Hueber F, Wepierre J, Schaefer H. Role of transepidermal and transfollicular routes in percutaneous absorption of hydrocortisone and testosterone: in vivo study in the hairless rat. *Skin Pharmacol*. 1992;5:99–107.
49. Illel, B., Schaefer, H., Wepierre, J. and Doucet, O. (1991) "Follicles play an important role in percutaneous absorption", J. Pharm. Sci. 80, 424–427.
50. Illel B, Schaefer H, Wepierre J, Doucet O. Follicles play an important role in percutaneous absorption. *J Pharm Sci*. 1991;80:424–427.
51. Indian British Pharmacopoeia 2009 British Pharmacopoeia Volume I & II Monographs: Medicinal and Pharmaceutical Substances Ciclopirox Olamine. 1334-1335.
52. Islam M, Reza S, Rahman H. In vitro Release Kinetics Study of Diltiazem Hydrochloride from Wax and Kollidon SR Based Matrix Tablets. Iranian Journal of Pharmaceutical Research. 2010; 7:101-8.
53. Jain A, Jain P, Kurmi J. Novel strategies for effective transdermal drug delivery: a review. Crit Rev Ther Drug Carrier Syst. 2014;31:219–272.
54. James WD, Berger T, Elston D. *Andrews' Diseases of the Skin*: *Clinical Dermatology*. 12th ed. Philadelphia: Elsevier; 2015.
55. J. Katsaras and T. Gutberlet, *Lipid Bilayers Structure and Interactions*, Springer, Berlin, Germany, 2001.
56. J. M. Seddon and R. H. Templer, "Polymorphism of lipid-water systems," in *Handbook of Biological Physics*, R. Lipowsky and E. Sackmann, Eds., vol. 1, chapter 3, pp. 97–160, Elsevier Science Publisher BV, 1995.
57. J. N. Israelachvili, "Thermodynamic and geometric aspects of amphiphile aggregation into micelles, vesicles and bilayers, and the interactions between them," in *Physics of Amphiphiles: Micelles, Vesicles and Microemulsions*, V. Degiorgio and M. Corti, Eds., pp. 24–58, North-Holland, Amsterdam, The Netherlands, 1985.
58. K. Holmberg, B. Jonsson, B. Kronberg, and B. Lindman, *Surfactants and Polymers in Aqueous Solution*, John Wiley & Sons, Chichester, UK, 2nd edition, 2002.
59. Kertész Z, Szikszai Z, Pelicon P, Sim i J, Telek A, Bíró T. Ion beam microanalysis of human hair follicles. Nucl Instrum Methods Phys Res B. 2007;260:218–221.
60. Kevin Garala, Parth Joshi, Malay Shah, A Ramkishan, Jaydeep Pate Formulation and evaluation of periodontal in situ gel. International Journal of Pharmaceutical Investigation. 2013; 3 (1): 29-41.
61. Knorr F, Lademann J, Patzelt A, Sterry W, Blume-Peytavi U, Vogt A. Follicular transport route – research progress and future perspectives. Eur J Pharm Biopharm. 2009;71:173–180.
62. Krause K, Foitzik K. Biology of the hair follicle: the basics. Semin Cutan Med Surg. 2006;25:2–10.
63. Kumar, Narendra,."Experimental investigation of PEG 6000/Tween 40/SiO2 NPs stabilized nanoemulsion properties: a versatile oil recovery approach." Journal of Molecular Liquids 319 (2020): 114087.
64. Kushnazarova, R.A.; Mirgorodskaya, A.B.; Lukashenko, S.S.; Voloshina, A.D.; Sapunova, A.S.; Nizameev, I.R.; Kadirov, M.K.; Zakharova, L.Y. Novel cationic surfactants bearing cleavable carbamate fragment: Tunable morphological behavior, solubilization of hydrophobic drugs and cellular uptake study. *J. Mol. Liq.* 2020, *318*, 113894. [Google Scholar]
65. Kwa'sniewska, D.; Chen, Y.-L.; Wieczorek, D. Biological activity of quaternary ammonium salts and their derivatives. *Pathogens* 2020, *9*, 459. [Google Scholar]
66. Lademann J, Otberg N, Richter H, et al. Investigation of follicular penetration of topically applied substances. Skin Pharmacol Appl Skin Physiol. 2000;14:17–22.
67. Lademann J, Richter H, Schaefer U, et al. Hair follicles – a long-term reservoir for drug delivery. *Skin Pharmacol Physiol*. 2006;19:232–236.
68. Lademann J, Weigmann HJ, Rickmeyer C, et al. Penetration of titanium dioxide microparticles in a sunscreen formulation into the horny layer and the follicular orifice. Skin Pharmacol Appl Skin Physiol. 1998;12:247–256.
69. Lauer AC, Lieb LM, Ramachandran C, Flynn GL, Weiner ND. Transfollicular drug delivery. Pharm Res. 1995;12:179–186.

70. Liaskoni, Athina, et al. "Paclitaxel controlled delivery using a pH-responsive functional-AuNP/block-copolymer vesicular nanocarrier composite system." European Journal of Pharmaceutical Sciences 117 (2018): 177-186.
71. M. J. Rosen, *Surfactants and Interfacial Phenomena*, Wiley, New York, NY, USA, 2nd edition, 1989.
72. Mahajan S, Chaudhari R, Patil V. Formulation and Evaluation of Topical Proniosomal Gel of Ciclopirox for Antifungal Therapy. ijpi [Internet]. 31Mar.2021 [cited 11May2023];11(1):56-2Naik A, Kalia YN, Guy RH. Transdermal drug delivery: overcoming the skin's barrier function. *Pharm Sci Technol Today*. 2000;3:318–326.
73. Meidan VM, Bonner MC, Michniak BB. Transfollicular drug delivery – is it a reality? Int J Pharm. 2005;306:1–14.
74. Meidan, V.M., Docker, M., Walmsley, A.D. and Irwin, W.J. (1998) "Low intensity ultrasound as a probe to elucidate the relative follicular contribution to total transdermal absorption", Pharm. Res. 15, 85–92
75. Meidan VM, Touitou E. Treatments for androgenetic alopecia and alopecia areata. *Drugs*. 2001;61:53–69
76. Mirgorodskaya, A.B.; Kushnazarova, R.A.; Lukashenko, S.S.; Voloshina, A.D.; Lenina, O.A.; Zakharova, L.Y.; Sinyashin, O.G. Carbamate-bearing surfactants: Micellization, solubilization, and biological activity. *J. Mol. Liq.* 2018, *269*, 203–210. [Google Scholar]
77. Mohammad F. Bostanudin Amphiphilic alkylated pectin hydrogels for enhanced topical drug delivery of fusidic Acid: Formulation and In Vitro Investigation Sci. Pharm. 2022, 90, 13
78. Montagna W. The Structure and Function of Skin. 3rd ed. New York: Academic Press; 1974.
79. Moscarella S. Therapeutic and antilipoperoxidant effects of silybin-phosphatidylcholine complex in chronic liver disease: Preliminary results. Curr. Ther. Res. 1993; 53(1): 98– 102.
80. National Center for Biotechnology Information (2023). PubChem Compound Summary for CID 2749, Ciclopirox. Retrieved May 9, 2023 from https://pubchem.ncbi.nlm.nih.gov/compound/Ciclopirox.
81. Nelson, D.L.; Cox, M.M. *Lehninger Principles of Biochemistry*, 7th ed.; Macmillan Publishers Ltd.: New York, NY, USA, 2017; 1312p. [Google Scholar]
82. Osborne D, Hatzenbuhler D. The influence of skin surface lipids on topical formulations. Drugs Pharm Sci. 1990;42:69–86.
83. Ossadnik M, Czaika V, Teichmann A, et al. Differential stripping: introduction of a method to show the penetration of topically applied antifungal substances into the hair follicles. *Mycoses*. 2007;50:457–462.
84. Otberg N, Richter H, Schaefer H, Blume-Peytavi U, Sterry W, Lademann J. Variations of hair follicle size and distribution in different body sites. J Invest Dermatol. 2004;122:14–19.
85. Otberg N, Teichmann A, Rasuljev U, Sinkgraven R, Sterry W, Lademann J. Follicular penetration of topically applied caffeine via a shampoo formulation. *Skin Pharmacol Physiol*. 2007;20:195–198.
86. Pandey A, Rath B, AK. D. Pharmaceutical Preformulation Studies with Special Emphasis on Excipients Compatibility. Chem Inform., 2012:43(23);20-5.
87. Para, G.; Łuczyn´ski, J.; Palus, J.; Jarek, E.; Wilk, K.A.; Warszyn´ski, P. Hydrolysis driven surface activity of esterquat surfactants. *J. Colloid Interface Sci.* 2016, *465*, 174–182. [Google Scholar]
88. Parul A. Ittadwar, Prashant K. Puranik. Novel umbelliferone phytosomes: development and optimization using experimental design approach and evaluation of photo-protective and antioxidant activity. International Journal of Pharmacy and Pharmaceutical Sciences. 2017; 9(1): 218-228.
89. Patzelt A, Knorr F, Blume-Peytavi U, Sterry W, Lademann J. Hair follicles, their disorders and their opportunities. Drug Discov Today Dis Mech. 2008;5:e173–e181.
90. Petrichenko, Oksana, et al. Evaluation of physicochemical properties of amphiphilic, 4-dihydropyridines and preparation of magnetoliposomes. *Nanomaterials* 11.3 (2021): 593.
91. Pi-Boleda, B.; Bouzas, M.; Gaztelumendi, N.; Illa, O.; Nogués, C.; Branchadell, V.; Pons, R.; Ortuño, R.M. Chiral pH-Sensitive cyclobutane β-amino acid-based cationic amphiphiles: Possible candidates for use in gene therapy. *J. Mol. Liq.* 2020, *297*, 111856. [Google Scholar]

92. Piérard-Franchimont C, Piérard G, Kligman A. Seasonal modulation of sebum excretion. Dermatology. 1990;181:21–22.
93. Polat BE, Figueroa PL, Blankschtein D, Langer R. Transport pathways and enhancement mechanisms within localized and non-localized transport regions in skin treated with low frequency sonophoresis and sodium lauryl sulfate. J Pharm Sci. 2011;100(2):512-29.
94. Polat BE, Hart D, Langer R, Blankschtein D. Ultrasoundmediated transdermal drug delivery: Mechanisms, scope, and emerging trends. J Control Release. 2011;152(3):330-48.
95. Poblet E, Ortega F, Jiménez F. The arrector pili muscle and the follicular unit of the scalp: a microscopic anatomy study. Dermatol Surg. 2002;28:800–803.
96. Prasanna Kumar Desu, G.Vaishnavi, K. Divya, U.Lakshmi. An Overview O Preformulation Studies. IAJPS 2015, 2 (10), 1399-1407.
97. Rancan F, Afraz Z, Combadiere B, Blume-Peytavi U, Vogt A. Hair follicle targeting with nanoparticles. In: Nasir A, Friedman A, Wang S, editors. Nanotechnology in Dermatology. Heidelberg: Springer; 2012:95–107.
98. Roque, Luís V.; Dias, Inês S.; Cruz, Nuno; Rebelo, Ana; Roberto, Amílcar; Rijo, Patrícia; Reis, Catarina P. (2017). Design of Finasteride-Loaded Nanoparticles for Potential Treatment of Alopecia. Skin Pharmacology and Physiology, (), 197–204.
99. Rostami, A.; Hashemi, A.; Takassi, M.A.; Zadehnazari, A. Experimental assessment of a lysine derivative surfactant for enhanced oil recovery in carbonate rocks: Mechanistic and core displacement analysis. *J. Mol. Liq.* 2017, *232*, 310–318. [Google Scholar]
100. Rusanov, A.I. *Micellization in Surfactant Solutions*; Taylor & Francis: London, UK, 1997; 326p. [Google Scholar]
101. Rutherford T, Black J. The use of autoradiography to study the localization of germicides in skin. Br J Dermatol. 1969;81:75–87.
102. S. C. Glotzer and M. J. Solomon, “Anisotropy of building blocks and their assembly into complex structures,” *Nature Materials*, vol. 6, no. 8, pp. 557–562, 2007.
103. Saad, A.H.; Kadhim, R.B.; Rasool, B. Formulation and evaluation of herbal shampoo from Ziziphus spina Christi leaves extract. Int. J. Res. Ayurveda Pharm., 2011, 2, 1802-1806.
104. Sanderson, J.E., Caldwell, R.W., Hsiao, J., Dixon, R. and Tuttle, R.R. (1987) “Noninvasive delivery of a novel iontropic catecholamine: iontophoresis versus intravenous infusion in dogs”, J. Pharm. Sci. 76, 215–218.
105. Senthil Kumar Rathnasamy, "Kinetics and optimization of microwave-assisted lignin fractionation with Protic low transition temperature mixture of Sesamum indicum straw for enhanced bioethanol production." Journal of Molecular Liquids 303 (2020): 112660
106. Schaefer H, Lademann J. The role of follicular penetration: a differential view. *Skin Pharmacol Appl Skin Physiol*. 2000;14:23–27.
107. Scheuplein, R.J. (1967) “Mechanism of percutaneous absorption II”, J. Investig. Dermatol. 48, 79–88.
108. Scheuplein RJ. Mechanism of percutaneous absorption. II. Transient diffusion and the relative importance of various routes of skin penetration. J Invest Dermatol. 1967;48:79–88.
109. Shirsand, Sidramappa.Ciclopirox olamine-loaded niosomal gel as a topical drug delivery system for fungal infections (2019).Vol. (2), 25-32.
110. Shreeraj H, Patil JKS, Patil NV. Gastroretentive drug delivery systems with potential herbal drugs for helicobacter pylori eradication: a review. J Chinese Integrative Med 2009; 7(10): 976-82.
111. Siddiqui, O., Sun, Y., Liu, J.-C. and Chien, Y.W. (1987) “Facilitated transdermal transport of insulin”, J. Pharm. Sci. 76, 341–345.
112. Suvarnalata Suhas Mahajan, RY Chaudhari, VR Patil Formulation and Evaluation of Topical Proniosomal Gel of Ciclopirox for Antifungal Therapy Int. J. Pharm. Investigation, 2021;11(1):56-62
113. Teichmann A, Otberg N, Jacobi U, Sterry W, Lademann J. Follicular penetration: development of a method to block the follicles selectively against the penetration of topically applied substances. *Skin Pharmacol Physiol*. 2005;19:216–223.
114. Thielitz A, Helmdach M, Röpke EM, Gollnick H. Lipid analysis of follicular casts from cyanoacrylate strips as a new method for studying therapeutic effects of antiacne agents. *Br J Dermatol*. 2001;145:19–27.

115. Tobin DJ. Biochemistry of human skin – our brain on the outside. Chem Soc Rev. 2006;35:52–67.
116. Tur E, Maibach H, Guy R. Percutaneous penetration of methyl nicotinate at three anatomic sites: evidence for an appendageal contribution to transport? Skin Pharmacol Physiol. 1991;4:230–234.
117. Umar H, Mahmood T, Hussain T, Aslam R, Shahzad Y, Yousaf AM. Formulation and In Vitro Characterization of Tea Tree Oil Anti-Dandruff Shampoo. Current Cosmetic Science. 2020;10(10):1-0.
118. Vanessa Alves Pinheiro, Daniela Serikaku, Andre Rolim Baby, Maria Vale´ria Robles Velasco, Telma Mary Kaneko, and Vladi Olga Consiglieri Development of ciclopirox olamine topical formulations: evaluation of drug release, penetration and cutaneous retention
119. Vogt A, Hadam S, Heiderhoff M, et al. Morphometry of human terminal and vellus hair follicles. Exp Dermatol. 2007;16:946–950.
120. Walters KA, Roberts MS. The structure and function of skin. *Drugs Pharm Sci*. 2002;119:1–40.
121. Wang, Y.; Yan, F.; Jia, Q.; Wang, Q. Quantitative structure-property relationship for critical micelles concentration of sugar-based surfactants using norm indexes. *J. Mol. Liq.* 2018, *253*, 205–210. [Google Scholar]
122. Washington N, Washington C, Wilson C. *Physiological Pharmaceutics*: *Barriers to Drug Absorption*. 2nd ed. London: Taylor & Francis; 2000.
123. Wester RC, Maibach HI. Regional variation in percutaneous absorption. Drugs Pharm Sci. 1999;97:107–116.
124. Whiting DA. Histology of normal hair. In: Hordinsky M, Sawaya ME, Scher RK, editors. Atlas of Hair and Nails. London: Churchill Livingstone; 1999:9–18.
125. Williams HC, Dellavalle RP, Garner S. Acne vulgaris. *Lancet*. 2012;379:361–372.
126. Wolf, J.D.; Kurpiers, M.; Baus, R.A.; Götz, R.X.; Griesser, J.; Matuszczak, B.; Bernkop-Schnürch, A. Characterization of an amino acid based biodegradable surfactant facilitating the incorporation of DNA into lipophilic delivery systems. *J. Colloid Interface Sci.* 2020, *566*, 234–241. [Google Scholar]
127. Wu, J.; Gao, H.; Shi, D.; Yang, Y.; Zhang, Y.; Zhu, W. Cationic gemini surfactants containing both amide and ester groups: Synthesis, surface properties and antibacterial activity. *J. Mol. Liq.* 2020, *299*, 112248. [Google Scholar]
128. Xia XR, Baynes RE, Monteiro-Riviere NA, Riviere JE. Determination of the partition coefficients and absorption kinetic parameters of chemicals in a lipophilic membrane/water system by using a membrane-coated fiber technique. Eur J Pharm Sci. 2005 Jan;24(1):15-23.
129. Yasa, S.R.; Kaki, S.S.; Poornachandra, Y.; Kumar, C.G.; Penumarthy, V. Synthesis, characterization, antimicrobial and biofilm inhibitory studies of new esterquats. *Bioorg. Med. Chem. Lett.* 2016, *26*, 1978–1982. [Google Scholar]
130. Yingjie Zhaia, Saisai Guoa, Chunhui Liub, Chunfen Yanga, Jinfeng Doua, Lingbing Li, Guangxi Zhai, Preparation and in vitro evaluation of apigenin-loaded polymeric micelles. Colloids and Surfaces A: Physicochem. Eng. Aspects 429 (2013) 24– 30.
131. Youcai, Z. "Chapter 3—biological treatment processes for leachate." *Pollution control technology for leachate from municipal solid waste. Elsevier, Amsterdam* (2018): 185-324.
132. Zakharova, L.Y.; Pashirova, T.N.; Doktorovova, S.; Fernandes, A.R.; Sanchez-Lopez, E.; Silva, A.M.; Souto, S.B.; Souto, E.B. Cationic surfactants: Self-assembly, structure-activity correlation and their biological applications. *Int. J. Mol. Sci.* 2019, *20*, 5534. [Google Scholar]
133. Zariwala, M. Gulrez, et al. Ascorbyl palmitate/DSPE-PEG nanocarriers for oral iron delivery: Preparation, characterisation and in vitro evaluation. Colloids and Surfaces B: Biointerfaces 115 (2014): 86-92.
134. Zheng, Y.; Zheng, M.; Ma, Z.; Xin, B.; Guo, R.; Xu, X. Sugar fatty acid esters. In *Polar Lipids: Biology Chemistry and Technology*; Academic Press and AOCS Press: Urbana, Italy, 2015; 568p. [Google Scholar]
135. Zhou, C.; Wang, Y. Structure–activity relationship of cationic surfactants as antimicrobial agents. *Curr. Opin. Colloid Interface Sci.* 2020, *45*, 28–43. [Google Scholar]